

1 **The Biogeophysical Climatic Impacts of Anthropogenic**  
2 **Land Use Change during the Holocene**

3  
4 **M. ~~Clare~~ Smith<sup>1</sup>, ~~Joy~~ S. Singarayer<sup>1</sup>, ~~Paul~~ J. Valdes<sup>2</sup>, ~~Jed~~ O. Kaplan<sup>3</sup>, ~~Nicholas~~  
5 ~~P. Branch~~<sup>4</sup>**

6 <sup>1</sup> Centre for Past Climate Change and Department of Meteorology, University of Reading,  
7 Reading, United Kingdom

8 <sup>2</sup> School of Geographical Sciences, University of Bristol, Bristol, United Kingdom

9 <sup>3</sup> Institute of Earth Surface Dynamics, University of Lausanne, Lausanne, Switzerland

10 <sup>4</sup> School of Archaeology, Geography and Environmental Science, University of Reading,  
11 Reading, United Kingdom

12

13 Correspondence to: M. Clare Smith (mcsmith@pgr.reading.ac.uk)

14

15 **Abstract**

16 The first agricultural societies were established around 10kaBP and had spread across much  
17 of Europe and southern Asia by 5.5kaBP with resultant anthropogenic deforestation for crop  
18 and pasture land. Various studies ([e.g. Joos et al., 2004](#), [Kaplan et al., 2011](#), [Mitchell et al.,](#)  
19 [2013](#)) have attempted to assess the biogeochemical implications for Holocene climate in  
20 terms of increased carbon dioxide and methane emissions. However, less work has been done  
21 to examine the biogeophysical impacts of this early land use change. In this study, global  
22 climate model simulations with HadCM3 were used to examine the biogeophysical effects of  
23 Holocene land cover change on climate, both globally and regionally, from the early  
24 Holocene (8 kaBP) to the early industrial era (1850 CE).

25 Two experiments were performed with alternative descriptions of past vegetation: (i) potential  
26 natural vegetation simulated by TRIFFID but no land-use changes, and (ii) where the  
27 anthropogenic land use model, KK10 (Kaplan et al., 2009, 2011) has been used to set the  
28 HadCM3 crop regions. Snapshot simulations have been run at 1000 year intervals to examine

1 when the first signature of anthropogenic climate change can be detected both regionally, in  
2 the areas of land use change, and globally. Results from our model simulations indicate that in  
3 regions of early land disturbance such as Europe and S.E. Asia detectable temperature  
4 changes, outside the normal range of variability, are encountered in the model as early as  
5 7kaBP in the June/July/August (JJA) season and throughout the entire annual cycle by 2-  
6 3kaBP. Areas outside the regions of land disturbance are also affected, with virtually the  
7 whole globe experiencing significant temperature changes (predominantly cooling) by the  
8 early industrial period. The global annual mean temperature anomalies were found to be  
9 -0.22°C at 1850 CE, -0.11°C at 2kaBP and -0.03°C at 7kaBP. Regionally, the largest  
10 temperature changes were in Europe with anomalies of -0.83°C at 1850 CE, -0.58°C at 2kaBP  
11 and -0.24°C at 7kaBP. Large-scale precipitation features such as the Indian monsoon, the  
12 intertropical convergence zone (ITCZ), and the North Atlantic storm track are also impacted  
13 by local land use and remote teleconnections. We investigated how advection by surface  
14 winds, mean sea level pressure (MSLP) anomalies, and tropospheric stationary wave train  
15 disturbances in the mid- to high-latitudes led to remote teleconnections.

16

## 17 **1 Introduction**

18 The first agricultural societies were established in the Near East around 10kaBP and had  
19 spread across most of Europe by 5.7kaBP (Zohary et al., 2012) and to India by 9kaBP  
20 (Tauger, 2013). In China domestication of millet and rice began about 8.5 kaBP initially  
21 spreading more slowly than in Europe but reaching S.E. Asia by 5.5kaBP (Roberts, 2013;  
22 Tauger, 2013). Agriculture was also independently developed in Mesoamerica with maize  
23 possibly being cultivated as far back as 9kaBP (Piperno et al., 2009) but, as in China, it spread  
24 slowly to other areas.

25 The most important anthropogenic alteration of the natural environment was the clearing of  
26 forests to establish cropland and pasture, and the exploitation of forests for fuel and  
27 construction materials (Darby, 1956). This long history of anthropogenic land ~~use~~-cover  
28 change (ALCC) has implications for regional hydrology and climate, and possibly for global  
29 climate. Deforestation results in both biogeochemical and biogeophysical changes. The  
30 biogeochemical changes tend to increase temperature by the emission of greenhouse gases  
31 such as CO<sub>2</sub> and CH<sub>4</sub> (CH<sub>4</sub> emissions are influenced not just directly by deforestation but by  
32 irrigation in rice agriculture and by emissions from livestock and humans). The impacts of

1 biogeophysical changes are many and varied, being dependent on the local climate, soil, and  
2 the natural vegetation that is being replaced, e.g. if natural savannah or grassland is replaced  
3 by crops the impact will not be as great as if woodland is replaced.

4 There are several mechanisms by which biogeophysical changes due to deforestation can  
5 affect regional climate. A combination of reduction in aerodynamic roughness, in the root  
6 extraction of moisture and in the capture of precipitation on the canopy leads to reduced  
7 evaporation and thus decreases the fluxes of moisture and latent heat from the surface to the  
8 atmosphere. These changes work to increase the local surface temperature (Lean and  
9 Rowntree, 1993). Conversely, the increase in surface albedo due to deforestation acts to  
10 decrease surface temperature by increasing the reflection of shortwave radiation. This is  
11 particularly true at high latitudes where lying snow is a factor for some of the year and the  
12 snow covered ground is no longer masked by the canopy of the forest. Generally, in mid to  
13 high latitudes the albedo increase is considered to be the dominant effect; leading to a net  
14 cooling of the regional surface temperature, whereas in the moist tropics the evaporation is  
15 more important and, therefore, a localised overall warming may result (Betts et al., 2006).

16 During the Holocene the climate has been influenced by natural forcings. Orbital variations  
17 have caused a decline in summer solar insolation in the Northern Hemisphere over the last  
18 6000 years. During the same period concentrations of greenhouse gases such as CO<sub>2</sub> and  
19 CH<sub>4</sub> have been increasing. On decadal to centennial timescales fluctuations in solar and  
20 volcanic activity have also had a climatic impact. (Wanner et al., 2008; Schmidt et al., 2011)  
21 The impact of ALCC is superimposed on these natural forcings. The extent and timing of  
22 these early anthropogenic land surface changes is the subject of much debate, as is their role  
23 in changing Holocene climate. Ruddiman (2003) proposed the idea that anthropogenic  
24 impacts on greenhouse gases, and consequently climate change, began thousands of years ago  
25 as a consequence of early agriculture and have been increasing in amplitude ever since, which  
26 he termed 'the early anthropogenic hypothesis'. The idea has been hotly debated in the  
27 literature (e.g. Broecker and Stocker, 2006; Joos et al., 2004; Singarayer et al., 2011; Mitchell  
28 et al., 2013; Kaplan et al., 2011). Whilst the early anthropogenic hypothesis may likely not  
29 account entirely for the pre-industrial rises in CO<sub>2</sub> and CH<sub>4</sub> there is no doubt that land use  
30 changes do have climatic impact on both regional and global scales. The real debate is the  
31 scale of these effects of early agriculture.

1 Whilst paleoecological and archaeological evidence of anthropogenic land use changes exists,  
2 there are not enough sites to comprehensively determine continental scale impacts of  
3 deforestation (Kaplan, 2009). Therefore, in order to better estimate impacts of anthropogenic  
4 land use, several databases of land use change have been developed. Examples of these  
5 include the HYDE 3.1 (History Database of the Global Environment, Goldewijk et al., 2011),  
6 KK10 (Kaplan et al., 2009 and 2011) and Pongratz et al. (2008) models. Although the  
7 methodologies differ in the details, the basic premise of these models is that from an  
8 estimated database of historical population trends, anthropogenic deforestation is calculated  
9 based on population density and the suitability of land for crops or pasture.

10 To quantify the impact of ALCC on climate, datasets of past ALCC can be used in  
11 conjunction with climate models. Several studies have estimated the influence of pre-  
12 industrial ALCC on global climate (He et al., 2014; Kutzbach, 2011; Pongratz et al., 2010).  
13 Globally, the biogeophysical effects of anthropogenic land use change have been estimated to  
14 cause a slight cooling that is offset by the biogeochemical warming, giving a net global  
15 warming (He et al., 2014; Pongratz et al., 2010). At the local to regional scale, in the most  
16 intensively altered landscapes of Europe, Asia, and North America, the biogeophysical effects  
17 can be comparable with the biogeochemical (He et al., 2014; Pongratz et al., 2010). In  
18 addition, Strandberg et al. (2014) used a regional climate model to evaluate the climatic effect  
19 of anthropogenic deforestation in Europe at 6kaBP and 0.2kaBP with both the HYDE 3.1 and  
20 KK10 ALCC scenarios. For the KK10 scenario at 6kaBP small but significant temperature  
21 differences were found in summer and, at 0.2kaBP, changes up to  $\pm 1$  °C were found over  
22 widespread areas in both summer and winter. Other authors (e.g. Oglesby et al., 2010; Cook  
23 et al., 2012) have modelled a decrease in precipitation in response to deforestation in  
24 Mesoamerica.

25 These existing studies are, however, limited in either temporal or spatial extent and do not  
26 address the question of when anthropogenically induced climate change first occurs. In this  
27 study global climate model simulations are used to provide a comprehensive evaluation of the  
28 influence that the biogeophysical effects of regional human-induced land cover change have  
29 had on the climate both globally and regionally throughout much of the Holocene. As  
30 described in detail in Sect. 2, the period under consideration is from 8kaBP to pre-industrial  
31 (1850) and snapshot simulations with HadCM3 were run at 1000-year intervals. The results  
32 are highlighted in Sect. 3. For evaluation purposes palaeoclimate reconstructions from

1 Bartlein et al .(2011) and Marcott et al .(2013) have been compared with the results from the  
2 model runs (Sect. 4). The implications are discussed in Sect. 5.

3

## 4 **2 Methodology**

### 5 **2.1 Model Description**

6 The climate simulations in this study were performed with the UK Hadley Centre coupled  
7 global climate model, HadCM3 (Gordon et al., 2000; Pope et al., 2000) with the Met Office  
8 Surface Exchange Scheme (MOSES2.1) (Essery, 2003) and TRIFFID (Top-down  
9 Representation of Interactive Foliage and Flora Including Dynamics) (Cox, 2001) dynamic  
10 vegetation. [The experimental set-up is summarised in Table 1.](#)

11 HadCM3, is a coupled atmospheric, ocean and sea ice model. The atmospheric component  
12 has a horizontal resolution of 2.5° latitude and 3.75° longitude with 19 unequally spaced  
13 levels in the vertical and a 30 minute time step. It has an Eulerian advection scheme and  
14 includes effects of CO<sub>2</sub>, N<sub>2</sub>O, CH<sub>4</sub>, CFC11 and CFC12. The spatial resolution over the ocean  
15 is 1.25° by 1.25° with 20 unequally spaced layers extending to a depth of 5,200m. It also  
16 includes a 1.25° by 1.25° resolution model for the formation of sea-ice with simple dynamics  
17 whereby the sea-ice drifts on the ocean currents (Cattle and Crossley 1995).

18 TRIFFID is coupled to the GCM (General Circulation Model) via MOSES every 10 days of  
19 the model run. Within TRIFFID nine surface types are specified: 5 plant functional types  
20 (PFTs) and 4 non-vegetation types.

21 HadCM3 was widely used in both the third and fourth assessment reports of the  
22 Intergovernmental Panel on Climate Change (IPCC, 2001, 2007) and still performs well in a  
23 number of tests relative to other global GCMs (Covey et al., 2003; IPCC, 2007). For the fifth  
24 IPCC assessment it has been superseded by HadGEM2 (Collins et al., 2011), but being  
25 relatively computationally efficient HadCM3 can be the better choice for some palaeoclimate  
26 modelling applications as it allows more and/or longer runs to be conducted than would be  
27 possible with a higher-resolution model.

28

## 1 2.2 Project-Specific Model Configuration

2 The version of HadCM3 used does not include interactive ice, carbon cycle, or methane and  
3 thus must be forced with prescribed changes in orbit, greenhouse gases and ice-sheet  
4 evolution. Orbital parameters are taken from Berger and Loutre (1991), atmospheric  
5 concentrations of gases are determined from ice cores (CO<sub>2</sub> from Vostok (Petit et al., 1999;  
6 Loulergue et al., 2008) and CH<sub>4</sub>, and N<sub>2</sub>O from EPICA (Spahni et al., 2005)) and the ice-  
7 sheet evolution is estimated using the ICE5G model of Peltier (2004). For further details of  
8 these natural forcings of the climate model readers are referred to Singarayer et al. (2011).

9 To prescribe Holocene ALCC the KK10 dataset of Kaplan et al. (2009 and 2011) was used.  
10 The original dataset is on a 5' spatial resolution and has modelled crop and pasture land use  
11 for every year from 8 kaBP to present. For this study the data at 1000-year intervals were  
12 taken (8kaBP, 7kaBP, etc.) for both crop and pasture combined and upscaled to the spatial  
13 resolution of HadCM3 to formulate a time series of cropland masks (Fig. 1). Within TRIFFID  
14 the global crop area is designated by a cropland mask, which can only be occupied by  
15 agricultural-type vegetation (i.e. C<sub>3</sub> and C<sub>4</sub> grasses) or bare soil (Betts et al., 2007). Hence, the  
16 actual cropland is equivalent to the mask area, less inland water, urban and ice tiles, and less  
17 the area covered by non-grassland vegetation or bare soil. The crop mask area is not  
18 dynamically updated by climate data. The cropland area incorporates the natural C<sub>3</sub>/C<sub>4</sub> grass  
19 fractional areas before converting tree fractions.

Formatted: Subscript

Formatted: Subscript

20 For each simulation, the boundary condition forcings (orbit, greenhouse gases and ice sheets)  
21 were specified, and in all simulations the initial conditions were the same, based on a spun-up  
22 early industrial simulation. Simulations were run for 1000 years. By the final 500 years of the  
23 simulation the climate system has adjusted to a new surface equilibrium and thus these final  
24 500 years were averaged to result in the mean altered climatic conditions. The relatively long  
25 averaging period increases the signal-to-noise ratio between the modified and control  
26 climates, and thus distinguishes differences that are statistically significant, but which can be  
27 hidden by decadal/multidecadal variability in shorter averaging periods. This is especially  
28 important for assessing the impact of agriculture in the earlier time slices of the Holocene  
29 when the land use change is small and localised.

30

## 1 3 Results

### 2 3.1 Surface Air Temperature

#### 3 3.1.1 Local Impacts of Land Use

4 In the regions where ALCC was significant, surface air temperature changes can be seen in all  
5 the time slice simulations (Figs. 2, 3 and 4) and for all time slices except 8kaBP (not shown)  
6 the temperature anomalies in most regions are outside the normal range of variability, which  
7 is considered to be within 2 standard deviations of the mean. The anomalies are more  
8 pronounced in the JJA season (Fig. 2) than DJF (Fig. 3). This is due to a combination of the  
9 land imbalance between the northern and southern hemispheres, the lack of land surface  
10 changes in the extra tropical southern hemisphere and the enhanced effect of land surface  
11 changes during the season of greatest solar insolation and plant growth (which is JJA in the  
12 northern hemisphere).

13 The direct temperature response to ALCC varies with the degree of latitude but the  
14 relationship is not straightforward as it depends on local climate, soil, and the natural  
15 vegetation. In the extratropics, where the albedo effect is generally dominant, there is a trend  
16 towards increasing (negative) anomalies with an increase in disturbance fraction (Fig. 4a-5a  
17 for P.I.). At 7kaBP the range of extra tropical temperature anomalies within the areas of land  
18 disturbance is +0.1/-1.2°C (JJA) and +0.6/-0.5°C (DJF), by 4kaBP it has increased to +0.4/-  
19 2°C (JJA) and +0.9/-1°C (DJF) and by the pre-industrial period (PI; 1850) it had reached  
20 +0.7/-4°C (JJA) and +0.3/-2°C (DJF). Although there are some positive temperature  
21 anomalies, the vast majority of grid points show a negative temperature trend. Regions with  
22 the highest ALCC intensity show the largest negative temperature anomalies, in particular  
23 Europe and E. Asia/China, where the agricultural land use occurs earliest and has the highest  
24 concentration of land conversion (Figs. 2, 3, 4 and 45a).

25 The tropical response shows less of a trend because the impact of reduced evaporation is more  
26 significant and thus there are conflicting signals between the cooling effect of increased  
27 albedo and the warming effect of reduced evaporation. In some tropical areas ALCC leads to  
28 net cooling while in other areas net warming is simulated (Figs. 2, 3, 4 and 54a), partly  
29 dependent on the availability of moisture at the surface and partly on cloud cover changes  
30 (not shown). The main areas that show a warm anomaly response are Southern Africa and  
31 India in JJA from 5kaBP and in DJF the area bordering the Bay of Bengal where E. India is

1 warmer from 6kaBP extending to the east coast of the Bay of Bengal by 2kaBP. The Indian  
2 JJA warming is enhanced by cloud feedbacks; a decrease in monsoon circulation leads to  
3 decreased cloudiness, thus increasing the shortwave radiation reaching the surface and  
4 warming the lower atmosphere. In contrast, tropical South America generally shows a net  
5 cooling in response to ALCC. Around the mid to late Holocene the tropical temperature  
6 anomaly range within the areas of land disturbance is  $\pm 0.5^{\circ}\text{C}$  and by the early industrial era  
7 (1850CE) it had reached  $\pm 1^{\circ}\text{C}$  (Fig. 45a).

8 Analysis of the standard deviation of both the KK10 and Control simulations indicated no  
9 significant changes in the amplitude of interannual variability of surface temperature or  
10 precipitation (using the F-test statistic).

### 11 3.1.2 Remote Impacts of Land Use

12 In addition to the local temperature changes described above, cooling can also be observed in  
13 regions remote from the areas of major ALCC, particularly in the Northern Hemisphere. The  
14 most intense cooling is always in the regions of ALCC but even as early as 7kaBP in the JJA  
15 season our model simulations show a band of cooling that stretches across much of the extra-  
16 tropical Northern Hemisphere and the North Atlantic (Fig. 2). This cooling starts influencing  
17 the northern Pacific regions by 5kaBP and by the early industrial era the surface air  
18 temperature over most of the world's land masses and much of the ocean is cooler due to the  
19 effects of ALCC in remote areas.

20 In the DJF season in the Northern Hemisphere ALCC leads to cooling both locally and  
21 regionally starting at 7kaBP (Fig. 3). The model simulations also show cooling in the Arctic  
22 and warming in Siberia. Cooling remote from the areas of major ALCC becomes more  
23 extensive by 3kaBP and most landmasses of the Northern Hemisphere are cooler than the  
24 control simulation by 2kaBP. The Siberian warm anomaly has ceased by 3kaBP but it remains  
25 less affected by the cooling than other regions. In the Southern Hemisphere, cooling remains  
26 more localised until 2kaBP by which time the majority of the land surface is cooler than the  
27 control.

28 There is an increased temperature anomaly response for the same level of disturbance fraction  
29 in the later timeslices (Fig. 4b5b) implying that the responses to the land use changes are not  
30 just due to the local effects. Some possible mechanisms for these remote impacts are large-  
31 scale circulation changes (such as stationary waves in the upper troposphere at mid-high



1 latitudes and monsoonal circulation changes), near-surface advection, and the amplifying  
2 factors of snow cover. These mechanisms will be discussed in more detail in Sect. 3.2 for  
3 atmospheric dynamics and Sect. 3.3.2 for snow cover changes. Changes to the natural  
4 vegetation cover (outside the regions of land use) due to the climatic impacts of land use were  
5 also investigated as a potential mechanism of further feedbacks but were not found to be  
6 significant.

## 7 **3.2 Atmospheric Dynamics**

### 8 **3.2.1 Upper Tropospheric Dynamics**

9 Cooler surface air temperature means that the density of the air is greater and, therefore, the  
10 geopotential height in cooler regions will be lower (See Fig. 67c and d). In the JJA season  
11 from 7kaBP there is a reduction of the 500hPa geopotential height over the extra-tropical  
12 Northern Hemisphere in a pattern similar to the temperature pattern but more extensive,  
13 completely encircling the globe. From 3kaBP onwards the height reduction expands  
14 southwards so the geopotential height is lowered almost everywhere by pre-industrial times.  
15 The most intense reduction is always in a zonal belt across Europe and E. Asia. The Southern  
16 Hemisphere response from 5kaBP appears to show a standing wave pattern affecting the  
17 subtropical highs.

18 In the DJF season a stationary wave in the anomaly field in both the Northern and Southern  
19 Hemispheres is apparent at all timeslices but most pronounced at 4kaBP (Fig. 67d). This is a  
20 recognised response to surface temperature anomalies as described in Hoskins and Karoly  
21 (1981) although, in this case, there are multiple thermal anomalies caused by ALCC. By  
22 2kaBP there is a reduction in 500hPa geopotential height over most of the globe. Note that  
23 there are several areas that are not statistically significant in Fig. 67c and d implying a large  
24 amount of variability. These geopotential height changes contribute to the simulated remote  
25 temperature changes by altering the regions of vorticity, which in turn influence the regions of  
26 ascent and descent and thus the surface climatic conditions. The geopotential height  
27 anomalies can also alter the pattern of the upper level winds thus influencing surface storm  
28 tracks.

29 In particular, the positioning of the geopotential height anomalies in the earlier timeslices (up  
30 to 4kaBP, Fig.67d) indicate an increased tendency towards a positive Tropical/ Northern  
31 Hemisphere (TNH) pattern (Barnston et al.,

1 [1991 http://www.epc.ncep.noaa.gov/data/teledoc/tmh.shtml](http://www.epc.ncep.noaa.gov/data/teledoc/tmh.shtml)) with above average heights over  
2 the Bering Strait/ Gulf of Alaska and northeastward of the Gulf of Mexico and below average  
3 heights over eastern Canada. This would be expected to cause cooler temperatures over the  
4 continental United States by increasing the transport of cold polar air into the United States.  
5 In several time slices it can be seen that DJF temperature anomalies over Bering Strait/Alaska  
6 (e.g. Fig. 3) show a warming pattern where there are positive geopotential height anomalies in  
7 Fig. 67c and d. The DJF temperature anomalies (warming) over Siberia up to 4ka (Fig. 3) also  
8 relate to the stationary wave pattern. The decreased heights over the polar regions in most of  
9 the time slices are indicative of a positive Arctic Oscillation (AO) (Fig. 67b) which has been  
10 shown to be correlated with milder winters in Siberia (Tubi and Dayan, 2012).

Formatted: Normal

12 The unequal latitudinal distribution of the temperature anomalies, with the regions of greatest  
13 cooling in the mid-latitudes of the Northern Hemisphere, affects the meridional temperature  
14 gradient leading to a change in baroclinicity, which has been shown to impact storm tracks  
15 (Yin, 2005).

Formatted: Normal

### 17 3.2.2 Mean Sea Level Pressure

Formatted: German (Germany)

#### 18 ~~3.2.2 Surface Advection~~

Formatted: Outline numbered +  
Level: 3 + Numbering Style: 1, 2, 3, ...  
+ Start at: 1 + Alignment: Left +  
Aligned at: 0 cm + Tab after: 1.27 cm  
+ Indent at: 1.27 cm

19 ~~Some of the cooling in regions remote from the areas of land disturbance is due to advection~~  
20 ~~by low level winds. In regions with a prevailing wind direction an advection pattern can be~~  
21 ~~clearly seen. Fig. 5 shows advection of cold air from the areas of land use change in East Asia~~  
22 ~~to the east across the West Pacific and from the region of land disturbance in Mexico to the~~  
23 ~~west across the East Pacific, this also affects the sea surface temperatures (SSTs) in these~~  
24 ~~regions of the Pacific (not shown). In other areas where the surface wind direction is more~~  
25 ~~variable the effect is more difficult to detect but probably does contribute to the spread of the~~  
26 ~~cold anomaly outward from the region of land disturbance.~~

Formatted: Normal

#### 27 ~~3.2.3 Mean Sea Level Pressure~~

Formatted: Normal

28 Changes to Mean Sea Level Pressure (MSLP) can also have an effect on the climate  
29 system. The colder surface air temperature in the region of disturbance means reduced ascent  
30 in those regions and thus higher MSLP. This can be seen quite clearly in China from 6ka and

1 | in Europe by 4kaBP (Fig. ~~5-6~~ for PI JJA), although the DJF situation in Europe is less  
2 | coherent probably due to more remote influences such as the North Atlantic storm track.  
3 | These MSLP changes could play a part in steering weather systems and thus influencing the  
4 | climate in remote regions. For example, the JJA MSLP anomaly pattern (Fig. ~~6a-7a~~ and b)  
5 | over the North and Central Atlantic is indicative of a negative phase of the North Atlantic  
6 | Oscillation (NAO) with above-normal pressure over the North Atlantic and below-normal  
7 | pressure over the central Atlantic. This pattern is apparent from 5kaBP. The NAO alters the  
8 | intensity and location of the North Atlantic jet stream and storm track and thus the patterns of  
9 | heat and moisture transport (Hurrell, 1995). A negative NAO would contribute to a tendency  
10 | to wetter summers in all but the southernmost regions of Europe (Folland et al., 2009) and this  
11 | was seen in the results described in Sect. 3.3.1. The DJF NAO shows a trend towards a  
12 | positive NAO which could result in drier winters over the Mediterranean region ([Hurrell et  
13 | al., 2003](http://www.epe.ncep.noaa.gov/data/teledoc/nao_pmap.shtml)[http://www.epe.ncep.noaa.gov/data/teledoc/nao\\_pmap.shtml](http://www.epe.ncep.noaa.gov/data/teledoc/nao_pmap.shtml)) ~~but although it is  
14 | difficult to ascertain whether this is the case as~~ the pattern is not as consistent as JJA.

### 15 | ~~3.2.4.3~~ **Surface Advection**

16 | ~~Some of the cooling in regions remote adjacent to from the areas of land disturbance is due to  
17 | advection by low-level winds. In regions with a prevailing wind direction an advection pattern  
18 | can be clearly seen. Fig. 56 shows advection of cold air from the areas of land use change in  
19 | East Asia to the east across the West Pacific and from the region of land disturbance in  
20 | Mexico to the west across the East Pacific, this also affects the sea surface temperatures  
21 | (SSTs) in these regions of the Pacific (not shown). In other areas where the surface wind  
22 | direction is more variable the effect is more difficult to detect but probably does contribute to  
23 | the spread of the cold anomaly outward from the region of land disturbance.~~

24 | **Formatted:** Indent: Left: 1.27 cm

### 25 | ~~3.2.5~~ **Upper Tropospheric Dynamics**

26 | ~~Cooler surface air temperature means that the density of the air is greater and, therefore, the  
27 | geopotential height in cooler regions will be lower (See Fig. 6c and d). In the JJA season from  
28 | 7kaBP there is a reduction of the 500hPa geopotential height over the extra-tropical Northern  
29 | Hemisphere in a pattern similar to the temperature pattern but more extensive, completely  
30 | encircling the globe. From 3kaBP onwards the height reduction expands southwards so the  
31 | geopotential height is lowered almost everywhere by pre-industrial times. The most intense~~

25 | **Formatted:** Normal

1 ~~reduction is always in a zonal belt across Europe & E. Asia. The Southern Hemisphere~~  
2 ~~response from 5kaBP appears to show a standing wave pattern affecting the subtropical high.~~  
3 ~~In the DJF season a stationary wave in the anomaly field in both the Northern and Southern~~  
4 ~~Hemispheres is apparent at all timeslices but most pronounced at 4kaBP (Fig. 6d). This is a~~  
5 ~~recognised response to surface temperature anomalies as described in Hoskins and Karoly~~  
6 ~~(1981) although, in this case, there are multiple thermal anomalies caused by ALCC. By~~  
7 ~~2kaBP there is a reduction in 500hPa geopotential height over most of the globe. Note that~~  
8 ~~there are several areas that are not statistically significant in Fig. 6e and d implying a large~~  
9 ~~amount of variability. These geopotential height changes contribute to the simulated remote~~  
10 ~~temperature changes by altering the regions of vorticity, which in turn influence the regions of~~  
11 ~~ascent and descent and thus the surface climatic conditions. The geopotential height~~  
12 ~~anomalies can also alter the pattern of the upper level winds thus influencing surface storm~~  
13 ~~tracks.~~  
14 ~~In particular, the positioning of the geopotential height anomalies in the earlier timeslices (up~~  
15 ~~to 4kaBP, Fig.6d) indicate an increased tendency towards a positive Tropical/ Northern~~  
16 ~~Hemisphere (TNH) pattern (<http://www.cpc.ncep.noaa.gov/data/teledoc/tmh.shtml>) with~~  
17 ~~above average heights over the Bering Strait/ Gulf of Alaska and northeastward of the Gulf of~~  
18 ~~Mexico and below average heights over eastern Canada. This would be expected to cause~~  
19 ~~cooler temperatures over the continental United States by increasing the transport of cold~~  
20 ~~polar air into the United States. In several time slices it can be seen that DJF temperature~~  
21 ~~anomalies over Bering Strait/Alaska (e.g. Fig. 3) show a warming pattern where there are~~  
22 ~~positive geopotential height anomalies in Fig. 6e and d. The DJF temperature anomalies~~  
23 ~~(warming) over Siberia up to 4ka (Fig. 3) also relate to the stationary wave pattern. The~~  
24 ~~decreased heights over the polar regions in most of the time slices are indicative of a positive~~  
25 ~~Arctic Oscillation (AO) (Fig. 6b) which has been shown to be correlated with milder winters~~  
26 ~~in Siberia (Tubi & Dayan, 2012).~~

### 28 3.3 Hydroclimate

29 Precipitation responses to ALCC (Fig. 7-8 for JJA and Fig. 8-9 for DJF) tend to be caused by  
30 a response to large-scale circulation changes rather than being directly attributable to local  
31 land use. The European precipitation response in the DJF season is not entirely consistent

1 throughout the time slices but the general response is a slight decrease in precipitation around  
2 the western and Mediterranean coasts with this dryness extending further into the continent by  
3 1 kaBP. The simulations show that Europe in the JJA season has an increase in precipitation  
4 compared to the control from 7kaBP onwards, which gradually increases in extent, possibly  
5 influenced by the increased tendency to a negative North Atlantic Oscillation (NAO). Positive  
6 anomalies begin in the warm pool of the Gulf of Mexico and extend across the North Atlantic  
7 following the track of positive anomalies to the 850hPa wind field (Fig. 910). In addition, as  
8 the cooler temperature anomalies extend quite high in the troposphere over Europe this  
9 increases relative humidity throughout the low to mid troposphere (not shown) and thus the  
10 likelihood of large-scale precipitation.

11 In India there is a decrease in monsoon precipitation from 5kaBP, which then gradually  
12 increases in intensity. This is partly driven by the slightly cooler Indian sub-continent  
13 temperatures (Fig. 4011) in the critical months for monsoon development and also by cooler  
14 temperatures in Europe and East Asia and increased snow cover on the Tibetan plateau. This  
15 leads to decreased monsoonal circulation and decreased cloudiness. There are also changes to  
16 the East Asian monsoon with wetter conditions to the north and south of the region and drier  
17 conditions in the centre. This pattern is seen reasonably consistently from 4kaBP onwards.

18 It should be noted that there are larger uncertainties in climate model simulated precipitation  
19 and other variables related to model dynamics than for temperature, which is primarily  
20 controlled by thermodynamics (Shepherd, 2014). Different climate models show a wide range  
21 of responses in their dynamics to palaeo and future climate change scenarios and we  
22 acknowledge that aspects of the precipitation anomaly patterns in this study may be less  
23 robust than that for other climate variables.

24

### 25 **3.3.1 Inter Tropical Convergence Zone (ITCZ)**

26 Analysis of the precipitation fields (Figs. 8-9 and 910) shows an overall southward migration  
27 of the ITCZ. These changes are most obvious in the Atlantic and Pacific Oceans and over the  
28 continent of Africa. In the DJF season there are changes to the ITCZ in the Western Pacific  
29 but a consistent pattern is not seen until 3ka when there is southward shift in the ITCZ over  
30 the Atlantic and Atlantic coasts leading by 2kaBP to a decrease in precipitation in the interior  
31 of southern Africa and wetter conditions on the coasts. There is generally increased

1 precipitation over the Indian Ocean and the Amazonian region of South America and a  
2 reduction over the Bay of Bengal but this pattern is not entirely consistent throughout the  
3 timeslices. Similarly, in the JJA season there are changes to the ITCZ throughout all the  
4 timeslices but these do not all show a consistent pattern. The most persistent changes are  
5 increased precipitation over the Pacific from 5kaBP, over Central America from 7kaBP and a  
6 southward shift from 2kaBP. This southward shift in the ITCZ in the JJA season impacts the  
7 West African monsoon with lower precipitation in a belt across the monsoon region by 2kaBP  
8 although the west coast of North Africa is wetter.

9 The generally cooler temperatures in the Northern Hemisphere may influence the latitudinal  
10 position of the Hadley cell and thus the location of the ITCZ via the influence on the inter-  
11 hemispheric temperature gradient resulting in the strengthening of the northward cross-  
12 equatorial energy transport (e.g. Kang et al., 2008). This shift south of the ITCZ to transport  
13 heat to the cooler northern hemisphere is seen in both the DJF and JJA seasons.

### 14 **3.3.2 Snow Cover**

15 Lower surface air temperatures in the ALCC scenario relative to the control lead to an  
16 increase in winter snow accumulation (Fig. 4.12). This increase is seen by 5kaBP mostly in  
17 northern and mountainous regions. The areas affected gradually increase so that by 3kaBP  
18 more temperate and lower lying areas see increases in snow depth. The effects are most  
19 pronounced in North America and Europe. In regions outside the areas of permanent snow  
20 cover increases in snow depth will delay the melting of the snow pack and thus result in a  
21 longer period of snow cover. The increased snow cover due to the cold temperature anomalies  
22 will cause additional cooling due to the increased albedo. This will be greatest in regions of  
23 deforestation where the snow-covered ground is no longer masked by the canopy of the  
24 forest. This increased snow cover would also lead to decreases in precipitation due to lower  
25 rates of moisture recycling over land.

26

## 27 **4 Temporal Evolution of Holocene Climate**

28 ~~The inclusion of land use changes through the Holocene has a significant impact on the~~  
29 ~~progression of global average temperatures, such as to alter the direction of the multi-~~  
30 ~~millennial trend.~~ In the control experiment the changes in orbital configuration, greenhouse  
31 gases (GHG), and icesheets/sea level lead to monotonically increasing global temperatures

1 | through the Holocene (Fig. [12a13a](#)). Analysis of previous experiments to assess the sensitivity  
2 | to different natural forcings (data from Singarayer and Valdes, 2010; Singarayer et al., 2011)  
3 | suggest that while the changes to orbital configuration effect a cooling in global temperature  
4 | over the Holocene, this is outweighed by increases in greenhouse gases (~17ppm CO<sub>2</sub> from  
5 | 8kaBP to late pre-industrial time), which result in overall warming. Cooling through the  
6 | Holocene occurs in northern hemisphere summer, when forced with orbit and GHG  
7 | variations, but is not as pronounced as when only forced by orbital variations. In winter, when  
8 | HadCM3 is forced with orbit-only variation there is little change in temperature, but when  
9 | GHG increases are included this becomes a warming over the Holocene, which then  
10 | outweighs the reduced summer cooling. Whilst ~~T~~this contrasts with recent data compilations  
11 | that suggest a general decline in global temperatures since the mid-Holocene (Marcott et al.,  
12 | 2013) it is within the range of other climate model responses when compared with the  
13 | Paleoclimate Model Intercomparison Project 3 (PMIP3) Mid-Holocene (MH) minus late Pre-  
14 | Industrial (PI) temperature anomalies.- Although palaeodata syntheses may suggest a cooling  
15 | of northern hemisphere temperatures, there are regional and seasonal variations in the data  
16 | such as that from the Bartlein et al.(2013) (Fig. 14c) and Mauri et al (2015) data compilations.  
17 | In both these compilations and the combined proxy reconstructions of Wanner et al. (2008)  
18 | the cooling is most evident over the higher latitude northern hemisphere.  
19 | The inclusion of land use changes through the Holocene has a significant impact on the  
20 | progression of modelled global average temperatures, such as to alter the direction of the  
21 | multi-millennial trend described above.The increasing magnitude and spread of ALCC  
22 | through the Holocene reconstructed in KK10 counteracts the influence of increasing  
23 | greenhouse gases, so that temperatures are effectively steady from 3kaBP in HadCM3 (Fig.  
24 | [13a14a](#)).

Formatted: Font color: Auto

Formatted: Font color: Auto

25 | These global trends are composed of considerable heterogeneity at the regional scale. When  
26 | broken down into zonal regions it can be clearly seen that the difference in trends  
27 | with/without land use is greatest in the Northern extratropics (Fig. [12b13b](#)), where the  
28 | Holocene trend is modified from increasing temperatures to decreasing temperatures in the  
29 | late Holocene by the addition of ALCC. There are impacts on mean temperatures in the  
30 | tropics (Fig. [12e13c](#)) and southern extratropics (Fig. [12d13d](#)) but not sufficient to influence  
31 | the direction of the Holocene trend.

1 | ~~Mid Holocene (MH)~~ minus ~~late Pre-Industrial (PI)~~ anomalies of annual mean surface air  
2 | temperature (Fig. ~~13a14a~~) show near global distribution of cooling, except over high latitude  
3 | sea-ice regions, which are particularly influenced by changes in obliquity (higher in the MH  
4 | than PI). The PMIP3 suite of models show a similar pattern of surface air temperature  
5 | anomalies. The cooling is most dramatic over the tropics and monsoonal regions, where  
6 | changes in the seasonality of insolation (due to orbital precession variation) intensify  
7 | monsoon circulation in the early and mid-Holocene and the resulting additional cloud cover  
8 | reduces incoming shortwave radiation as well as increased surface water altering the balance  
9 | of sensible to latent heat fluxes. The inclusion of land use change in the KK10 experiment  
10 | reduces the magnitude of MH cooling, especially in the mid-latitudes. Over Europe and  
11 | eastern North America the anomaly is reversed to a warming (i.e. over these regions the  
12 | cooling from deforestation shown in Fig. 2, increases and outstrips the warming from  
13 | greenhouse gases). These are also regions where there is the highest concentration of pollen  
14 | reconstructions (Fig. ~~13e14c~~; Bartlein et al., 2011; Mauri et al., 2014). The influence of land  
15 | use change improves the data-model comparison with the reconstruction by Bartlein et al.  
16 | (2011) over these key areas (Fig. ~~13a14a-c~~). Likewise, when simulated top-level ocean  
17 | temperatures are compared with SST data used within the Marcott et al. (2013) compilation,  
18 | the inclusion of land use improves the data-model comparison (Fig. ~~13d-14d~~ and e). However,  
19 | the largest MH warming in the model is in the summer months, whereas, recent seasonal  
20 | temperature reconstructions (also using pollen; Mauri et al., 2014) suggest the largest and  
21 | most widespread MH warming may have occurred in winter in the MH.

22 | In contrast, using the KK10 ALCC scenario as a boundary condition to the climate model  
23 | does not improve the agreement in annual mean MH - PI precipitation anomalies when  
24 | compared to the palaeoclimate reconstruction of Bartlein et al. (2011) (Fig. ~~1415~~). Model and  
25 | data are in reasonable agreement in most regions except for Europe and the temperate regions  
26 | of Asia where the data implies a wetter MH than PI, which is not seen in the model runs. The  
27 | difference over Europe is exacerbated by the inclusion of land use, which results in a drier  
28 | MH.

29

## 30 | **5 Discussion**

31 | Anthropogenic land cover change leads to climate change well beyond the core regions of  
32 | land use early in the Holocene. These results suggest that regional ALCC has an effect on the



1 atmospheric circulation, e.g. the ITCZ shift is a remote response on global scale. The  
2 implications of this finding are that regional models or atmospheric-only models would not  
3 simulate these atmospheric circulation changes as well as a global coupled model. In this  
4 study we observed multiple thermal anomalies (from intense regions of cooling directly over  
5 anthropogenic land use change), but the standing wave response of the geopotential height  
6 field would likely also be seen even for a single thermal source from just one region (Hoskins  
7 and Karoly, 1981). ~~A R~~regional models have the advantages of higher spatial resolution and  
8 more detailed orography but they may not include these potential remote atmospheric changes  
9 (e.g. Strandberg et al., 2014) and may possibly resulting in different impacts from the same  
10 land cover forcing ~~for in~~ regional and global model simulations. The positioning of the major  
11 temperature anomalies in the mid-latitudes and at similar latitudes may be particularly  
12 significant in producing the stationary wave pattern.

13 Whilst these are the results from only one model there are many similarities in the distribution  
14 of the temperature anomalies with those found by He et al. (2014) for 1850 CE and Pongratz  
15 et al. (2010) for the 20th century although the temperature changes found in this study were  
16 greater e.g. a pre-industrial global annual mean temperature anomaly of  $-0.23^{\circ}\text{C}$  as opposed to  
17 the  $-0.17^{\circ}\text{C}$  estimated by He et al. (2014). Running similar simulations with a greater number  
18 of models would improve the robustness of the results particularly with respect to  
19 hydroclimate due to the high uncertainties involved. The was the variability in the results from  
20 different models can be greater than the variability of the property that is being assessed  
21 (Pitman et al., 2009; de Noblet-Ducoudre et al., 2012; Brovkin et al., 2013). These  
22 inconsistencies have been attributed to disagreements in how land use change is implemented,  
23 the parameterisation of albedo, the representation of crop phenology and evapotranspiration  
24 and the partitioning of available energy between latent and sensible heat fluxes (Pitman et al.,  
25 2009; de Noblet-Ducoudre et al., 2012; Boisier et al., 2012). The albedo and turbulent heat  
26 fluxes from our model simulations for the North America/Eurasia region (Fig. 16) are  
27 within the range of other climate model responses when compared with those from the Land-  
28 Use and Climate, IDentification of robust impacts (LUCID) set of experiments (Boisier,  
29 2012). The negative turbulent and latent heat fluxes would offset some of the cooling due to  
30 the increased albedo. Although the largest albedo changes are in the DJF season the impact of  
31 this will be lessened the due to the lower levels of incoming solar radiation in this season.  
32 ~~R~~The results could be further improved by the running of transient simulations that could  
33 capture events such as the Maunder minimum. ~~This was included in the 0.2kaBP simulations~~

Formatted: Font color: Text 1

Formatted: Font color: Text 1

1 ~~of Strandberg et al. (2014):~~ A transient simulation response could result in different  
2 biogeophysical impacts to the ones achieved when using a long equilibrium simulation where  
3 the ocean-land-atmosphere system can reach more of a steady state and the climate sensitivity  
4 is different.

5 From late preindustrial era simulations, one using observed atmospheric greenhouse gas  
6 concentrations and the other using greenhouse gas concentrations in a world with no  
7 anthropogenic emissions (based on linear projection from earlier Holocene trends from  
8 Kutzbach et al., 2011), He et al. (2014) estimated a net global warming of 0.9°C due to the  
9 biogeochemical effects of ALCC, with between 0.5 and 1.5°C warming in the areas of most  
10 intense land use changes. Incorporating this degree of warming into our early industrial era  
11 (1850 CE) simulations there would still be a net cooling in Europe, E. Asia and N.E. America  
12 with, e.g., a net cooling of up to 2°C in parts of Europe. To put this in perspective the IPCC  
13 (IPCC WG II, 2014a) consider a temperature rise of more than 2°C to be undesirable and that  
14 changes of 1°C could have an impact on vulnerable ecosystems. However, the temperature  
15 changes in this study took place over a much longer period than the timeframe considered in  
16 the IPCC and ecosystems and human societies would have had more time to adapt. The  
17 consequences of these changes for agricultural societies would vary depending on the pre-  
18 existing conditions. For example, in drier regions, where crops are more likely to be water  
19 limited, cooler, wetter summer conditions may have been beneficial to the agricultural output  
20 although the risk of erosion would be increased. The generally lower temperatures might also  
21 make societies more vulnerable to further transient cooling effects such as volcanic activity.

22 There are discrepancies between simulations of the mid-Holocene climate and the  
23 independent data-based reconstructions. Both the simulations from this study and virtually all  
24 the PMIP3 (Palaeoclimate Model Intercomparison 3; <https://pmip3.lsce.ipsl.fr>) models show a  
25 temperature increase from the mid-Holocene to the PI whereas the Marcott et al. (2013) (and  
26 Mann et al. (2008) on a shorter timescale) reconstructions show a decrease. It is interesting to  
27 note that ALCC reduces this mismatch for HadCM3, especially in key areas such as Europe.  
28 Other factors that could lead to this discrepancy are uncertainties in the proxy reconstructions  
29 and deficiencies in climate models. These climate model deficiencies include low resolution  
30 and sensitivity and, importantly, their dependence on soil moisture whereby energy is utilised  
31 for evaporation rather than for temperature increase.

1 This study shows a significant increase in precipitation over Europe with increasing land use  
2 which means that the PI becomes wetter than the mid-Holocene, which leads to increases in  
3 soil moisture and changes in the sensible to latent heat flux balance and, in combination with  
4 increased albedo caused by deforestation, this results in cooler temperatures for PI than MH.  
5 If the land-atmosphere coupling strength was different and soil moisture was strongly reduced  
6 with deforestation it is likely that the cooling effect would be smaller (cf. Strandberg, 2014).

7 Further uncertainties arise from the robustness of the land use reconstructions, which is  
8 difficult to evaluate due to the lack of global-scale evidence for human impact on the Earth's  
9 land surface. Much of the uncertainty comes from the lack of knowledge about the magnitude  
10 and distribution of the global human population and the rate of technological evolution and  
11 intensification through time. As part of our initial investigations simulations were also run  
12 using an alternative land use scenario (the HYDE 3.1 dataset; Goldewijk et al., 2011). The  
13 HYDE 3.1 reconstruction has substantially lower levels of land use early in the Holocene (as  
14 compared with KK10), which resulted in a later development of consistent temperature  
15 anomalies at 4kaBP (not shown) in comparison with the KK10 land use scenario. The  
16 decision was taken to proceed with the KK10 data due to its assumptions of a larger per capita  
17 land use earlier in the Holocene when agricultural methods were less efficient. Several  
18 ongoing international initiatives that aim to synthesise palaeoecological and archaeological  
19 data promise to lead to more robust reconstructions of Holocene ALCC in the future (e.g.  
20 PAGES LandCover6k project; <http://www.pages-igbp.org/workinggroups/landcover6k/intro>).

21 By the early industrial period simulated biogeophysical temperature changes in the regions of  
22 land disturbance are of the same order of magnitude (e.g. 0.83°C annual anomaly in the main  
23 agricultural areas of Europe) as the changes seen due to CO<sub>2</sub> increases during the industrial  
24 period (0.85°C, IPCC synthesis report, 2014b). Part of Ruddiman's original hypothesis  
25 (Ruddiman, 2003) is that pre-industrial global warming caused by anthropogenic CO<sub>2</sub>/CH<sub>4</sub>  
26 emissions should have been ~2 °C at higher latitudes, but there was no evidence for this  
27 warming. Ruddiman (2003) attributed this to a natural cooling trend caused by decreasing  
28 summer insolation. This study suggests that biogeophysical effects of the land use changes  
29 may also have played a part in counteracting the warming due to anthropogenic greenhouse  
30 gas emissions as acknowledged in Ruddiman (2013). The precipitation changes might also  
31 have an impact on the availability of water for rice irrigation and on natural wetlands thus  
32 affecting the production of methane.

1

## 2 **6 Conclusions**

3 In our global model simulations that use a Holocene ALCC scenario as a boundary condition,  
4 a surface temperature response to the biogeophysical effects of ALCC is seen in regions of  
5 early land use such as Europe and S.E. Asia as early as 7kaBP in the JJA season and  
6 throughout the entire annual cycle by 2-3kaBP. Areas outside the major regions of ALCC are  
7 also affected, with virtually the whole globe experiencing significant temperature changes  
8 with a net global cooling of 0.2322°C by the pre-industrial period. Although the temperature  
9 changes are predominantly cooling some regions such as India, Southern Africa and Siberia  
10 show warming as a response to ALCC. The greatest changes are generally seen in the JJA  
11 season with a mean regional cooling of 1.4°C experienced in Europe and 1°C in E. Asia in the  
12 early industrial period (1850 CE). Much of the precipitation response to the land use tends to  
13 be due to large-scale circulation changes such as a decrease in the intensity of the Indian  
14 monsoon, the southward movement of the ITCZ and changes to the North Atlantic storm  
15 track. In Europe there is a slight decrease in precipitation in the DJF season and a more  
16 substantial increase in the JJA season. Some causal factors for the teleconnections are  
17 advection by surface winds, MSLP anomalies, and tropospheric stationary wave train  
18 disturbances in the mid- to high-latitudes.

19 The potential for an early global impact of ALCC on climate strongly implied by this study  
20 suggests that due consideration of this should be taken in simulations covering the Holocene.  
21 The inclusion of ALCC in the model improves the model comparison for surface air  
22 temperature with the data-driven palaeoclimate reconstructions especially in key areas such as  
23 Europe. The remote teleconnections seen in this study have implications for the regional  
24 modelling of land use change due to circulation changes that occur outside the domain of the  
25 regional model.

26 Overall, our model simulations indicate an increase in global surface air temperatures through  
27 the Holocene. Globally, the inclusion of ALCC data reduces the magnitude of this warming  
28 especially in the late Holocene when the temperatures remain relatively constant. Regionally,  
29 in the Northern extratropics, this warming is reversed in the late Holocene. It should be noted  
30 that in this study it is not possible to distinguish the anthropogenic component of the  
31 biogeochemical changes as the same atmospheric CO<sub>2</sub> and CH<sub>4</sub> concentrations (from ice core  
32 measurements) are prescribed for both the KK10 and control simulations. However, the level

1 of early industrial warming due to the biogeochemical impacts of ALCC predicted by He et  
2 al. (2014) would negate the early industrial biogeophysical cooling seen in this study in all  
3 regions except for the most intensively altered landscapes of Europe, E. Asia and N.E.  
4 America.

5 Other caveats are the large uncertainties in the land use data and, therefore, in our  
6 understanding of the Holocene evolution of land surface-climate interactions as well as our  
7 ability to evaluate climate models. To reduce these uncertainties there is an urgent need to  
8 extend land cover reconstructions and prehistory of land use globally (cf. LandCover6k  
9 PAGES initiative).

10

11

## 12 **Data Availability**

13 Data is available from the Bristol Research Initiative for the Dynamic Global Environment  
14 website: <http://www.bridge.bris.ac.uk/resources/simulations>

15

## 16 **Acknowledgements**

17 MCS is supported by a University of Reading doctoral scholarship. MCS and JSS would like  
18 to thank Sandy Harrison and Beni Stocker for useful discussions on land cover  
19 reconstructions. JOK was supported by the European Research Council (313797  
20 COEVOLVE)

21

## References

Barnston, A., Livezy, R., and Halpert, M.: Modulation of southern oscillation northern-hemisphere midwinter climate relationships by the QBO, J. Climate, 4, 203-217, 1991.

Bartlein, P.J., Harrison, S.P., Brewer, S., Connor, S., Davis, B.A.S., Gajewski, K., Guiot, J., Harrison-Prentice, T.I., Henderson, A., Peyron, O., Prentice, I.C., Scholze, M., Seppä, H., Shuman, B., Sugita, S., Thompson, R.S., Viau, A.E., Williams, J. and Wu, H.: Pollen-based continental climate reconstructions at 6 and 21 ka: a global synthesis, *Clim. Dynam.*, 37, 775-802, doi:10.1007/s00382-010-0904-1, 2011.

Berger, A., and Loutre, M. F.: Insolation values for the climate of the last 10 million years, *Quaternary Sci. Rev.*, 10, 297-317, doi:10.1016/0277-3791(91)90033-Q, 1991.

Betts, R. A., Falloon, P. D., Goldewijk, K. K., and Ramankutty, N.: Biogeophysical effects of land use on climate: Model simulations of radiative forcing and large-scale temperature change, *Agr. Forest Meteorol.*, 142, 216-233, doi:10.1016/j.agrformet.2006.08.021, 2007.

Boisier, J. P., de Noblet-Ducoudré, N., Pitman, A.J., Cruz, F.T., Delire, C., den Hurk, B.J.J.M., Molen, M.K., Müller, C. and Voldoire, A.: Attributing the impacts of land-cover changes in temperate regions on surface temperature and heat fluxes to specific causes: Results from the first LUCID set of simulations, J. Geophys. Res.-Atmos., 117, doi:http://dx.doi.org/10.1029/2011JD017106, 2012

Broecker, W.S. and Stocker, T.F.: The Holocene CO2 rise: Anthropogenic or natural?, *Eos Trans. AGU*, 87, 27-27, doi:10.1029/2006EO030002, 2006.

Brovkin, V., Boysen, L., Arora, V. K., Boisier, J. P., Cadule, P., Chini, L., Claussen, M., Friedlingstein, P., Gayler, V., Hurk, v.d., B.J.J.M, Hurtt, G.C., Jones, C.D., Kato, E., Noblet-Ducoudré, d., N., Pacifico, F., Pongratz, J. and Weiss, M.: Effect of anthropogenic land-use and land-cover changes on climate and land carbon storage in CMIP5 projections for the twenty-first century. *J. Climate*, 26, 6859, 2013.

Collins, W.J., Bellouin, N., Doutriaux-Boucher, M., Gedney, N., Halloran, P., Hinton, T., Hughes, J., Jones, C.D., Joshi, M., Liddicoat, S., Martin, G., O'Connor, F., Rae, J., Senior, C., Sitch, S., Totterdell, I., Wiltshire, A. and Woodward, S.: Development and evaluation of an Earth-system model – HadGEM2, *Geosci. Model Dev.*, 4, 1051-1075, doi:10.5194/gmdd-4-1051-2011, 2011.

Formatted: Font: (Default) Times New Roman, Not Bold

Formatted: Font: Not Bold

Formatted: Font: (Default) Times New Roman, Not Bold

Formatted: Font: Not Bold

Formatted: Font: (Default) Times New Roman, Not Bold

1 Cook, B. I., Anchukaitis, K. J., Kaplan, J. O., Puma, M. J., Kelley, M., and Gueyffier, D.:  
2 Pre-Columbian deforestation as an amplifier of drought in Mesoamerica, *Geophys. Res. Lett.*,  
3 39, L16706, doi:10.1029/2012GL052565, 2012.

4 Covey, C., AchutaRao, K.M., Cubasch, U., Jones, P., Lambert, S.J., Mann, M.E., Phillips,  
5 T.J. and Taylor, K.E.: An overview of results from the Coupled Model Intercomparison  
6 Project, *Global Planet. Change*, 37, 103-133, doi:10.1016/S0921-8181(02)00193-5, 2003.

7 Cox, P.M.: Description of the TRIFFID dynamic global vegetation model. Cox, P. M., Tech.  
8 Note 24, Hadley Centre, Met Office, 16 pp, available at <http://www.metoffice.gov.uk>, (last  
9 access 15 September 2015), 2001.

10 Darby, H.C.: The clearing of the woodland in Europe. In: *Man's Role in Changing the Face of*  
11 *the Earth*, edited by Thomas Jr., W.L., University of Chicago Press, Chicago, 183-216, 1956.

12 de Noblet-Ducoudré, N., Pitman, A., Delire, C., Hurk, v. d., B.J.J.M., Boisier, J. P., Brovkin,  
13 V., Cruz, F., Voltaire, A., Molen, v.d., M.K., Müller, C., Bonan, G.B., Gayler, V., Reick,  
14 C.H., Strengers, B.J. and Lawrence, P. J.: Determining robust impacts of land-use induced  
15 land-cover changes on surface climate over North America and Eurasia; results from the first  
16 set of LUCID experiments. *J. Climate*, 25, 3261-3281, 2012.

17 Essery, R. L. H., Best, M. J., Betts, R. A., Cox, P. M., and Taylor, C. M.: Explicit  
18 representation of subgrid heterogeneity in a GCM land surface scheme, *J. Hydrometeorol.*, 4,  
19 530-543, doi:10.1175/1525-7541(2003)004<0530:EROSHI>2.0.CO;2, 2003.

20 Folland, C.K., Knight, J., Linderholm, H.W., Fereday, D., Ineson, S., and Hurrell, J.W.: The  
21 Summer North Atlantic Oscillation: Past, Present, and Future, *J. Climate*, 22, 1082-1103.  
22 doi:10.1175/2008JCLI2459.1, 2009.

23 Goldewijk, K. K., Beusen, A., Van Drecht, G., and De Vos, M.: The HYDE 3.1 spatially  
24 explicit database of human-induced global land-use change over the past 12,000 years, *Global*  
25 *Ecol. Biogeogr.*, 20, 73-86, doi:10.1111/j.1466-8238.2010.00587, 2011.

26 Gordon, C., Cooper, C., Senior, C.A., Banks, H., Gregory, J.M., Johns, T.C., Mitchell, J.F.B.  
27 and Wood, R.A.: The simulation of SST, sea ice extents and ocean heat transports in a version  
28 of the Hadley Centre coupled model without flux adjustments, *Clim. Dynam.*, 16, 147-168,  
29 doi:10.1007/s003820050010, 2000.

1 He, F., Vavrus, S. J., Kutzbach, J. E., Ruddiman, W. F., Kaplan, J. O. and Krumhardt, K. M.:  
2 Simulating global and local surface temperature changes due to Holocene anthropogenic land  
3 cover change, *Geophys. Res. Lett.*, 41, 623-631, 2014.

4 Hoskins, B. J., and Karoly, D. J.: The steady linear response of a spherical atmosphere to  
5 thermal and orographic forcing, *J. Atmos. Sci.*, 38, 1179-1196, 1981.

6 Hurrell, J. W. : Decadal trends in the north Atlantic oscillation: Regional temperatures and  
7 precipitation. *Science*, 269, 676-679. doi:10.1126/science.269.5224.676, 1995.

8 [Hurrell, J. W., Kushnir, Y., Ottersen, G., and Visbeck, M.: An Overview of the North Atlantic](#)  
9 [Oscillation, in \*The North Atlantic Oscillation: Climatic Significance and Environmental\*](#)  
10 [Impact edited by Hurrell, J. W., Kushnir, Y., Ottersen, G., and Visbeck, M., \*Am. Geophys.\*](#)  
11 [Union, Washington, D. C., doi: 10.1029/134GM01, 2003](#)

12 Intergovernmental Panel on Climate Change (IPCC): Impacts, Adaptation and Vulnerability –  
13 Contribution of Working Group II to the Third Assessment Report of IPCC, Cambridge  
14 University Press, 2001.

15 Intergovernmental Panel on Climate Change (IPCC): The Physical Science Basis –  
16 Contribution of Working Group I to the Fourth Assessment Report of the IPCC, Cambridge  
17 University Press, 2007.

18 IPCC, 2014: Climate Change 2014: Impacts, Adaptation, and Vulnerability. Part A: Global  
19 and Sectoral Aspects. Contribution of Working Group II to the Fifth Assessment Report of  
20 the Intergovernmental Panel on Climate Change edited by: Field, C.B., Barros, V.R.,  
21 Dokken, D.J., Mach, K.J., Mastrandrea, M.D., Bilir, T.E., Chatterjee, M., Ebi, K.L., Estrada,  
22 Y.O., Genova, R.C, Girma, B., Kissel, E.S., Levy, A.N., MacCracken, S., Mastrandrea, P.R.,  
23 and White, L.L., Cambridge University Press, Cambridge, United Kingdom and New York,  
24 NY, USA, 1132 pp., 2014a.

25 IPCC, 2014: Climate Change 2014: Synthesis Report. Contribution of Working Groups I, II  
26 and III to the Fifth Assessment Report of the Intergovernmental Panel on Climate Change,  
27 edited by Core Writing Team, Pachauri, R.K. and Meyer, L.A. , IPCC, Geneva, Switzerland,  
28 151 pp., 2014b.

29 Joos, F., Gerber, S., Prentice, I. C., Otto-Bliesner, B. L., and Valdes, P. J.: Transient  
30 simulations of Holocene atmospheric carbon dioxide and terrestrial carbon since the last  
31 glacial maximum, *Global Biogeochem. Cy.*, 18, GB2002. doi:10.1029/2003GB002156, 2004.



1 Kang, S. M., Held, I. M., Frierson, D. M., and Zhao, M.: The response of the ITCZ to  
2 extratropical thermal forcing: Idealized slab-ocean experiments with a GCM, *J. Climate*, 21,  
3 3521-3532, 2008.

4 Kaplan, J. O., Krumhardt, K. M., and Zimmermann, N.: The prehistoric and preindustrial  
5 deforestation of Europe, *Quaternary Sci. Rev.*, 28, 3016-3034.  
6 doi:10.1016/j.quascirev.2009.09.028, 2009.

7 Kaplan, J. O., Krumhardt, K. M., Ellis, E. C., Ruddiman, W. F., Lemmen, C., and Goldewijk,  
8 K. K.: Holocene carbon emissions as a result of anthropogenic land cover change, *Holocene*,  
9 21, 775-791, doi:10.1177/0959683610386983, 2011.

10 Kutzbach, J. E., Vavrus, S. J., Ruddiman, W. F., and Philippon-Berthier, G.: Comparisons of  
11 atmosphere-ocean simulations of greenhouse gas-induced climate change for pre-industrial  
12 and hypothetical 'no-anthropogenic' radiative forcing, relative to present day, *Holocene*, 21,  
13 793-801, doi:10.1177/0959683611400200, 2011.

14 Lean, J., and Rowntree, P. R.: A GCM simulation of the impact of Amazonian deforestation  
15 on climate using an improved canopy representation, *Q. J. Roy. Meteor. Soc.*, 119, 509-530.  
16 doi:10.1002/qj.49711951109, 1993.

17 Loulergue, L., Schilt, A., Spahni, R., Masson-Delmotte, V., Blunier, T., Lemieux, B.,  
18 Barnola, J., Raynaud, D., Stocker, T.F. and Chappellaz, J.: Orbital and millennial-scale  
19 features of atmospheric CH<sub>4</sub> over the past 800000 years, *Nature*, 453, 383-386,  
20 doi:10.1038/nature06950, 2008.

21 Mann, M. E., Zhang, Z., Hughes, M. K., Bradley, R. S., Miller, S. K., Rutherford, S., and Ni,  
22 F.: Proxy-based reconstructions of hemispheric and global surface temperature variations over  
23 the past two millennia, *P. Natl. Acad. Sci. USA*, 105, 13252-13257,  
24 doi:10.1073/pnas.0805721105, 2008.

25 Marcott, S. A., Shakun, J. D., Clark, P. U., and Mix, A. C.: A reconstruction of regional and  
26 global temperature for the past 11300 years, *Science*, 339, 1198-1201,  
27 doi:10.1126/science.1228026, 2013.

28 Mauri, A., Davis, B. A. S., Collins, P. M., and Kaplan, J. O.: The climate of Europe during  
29 the Holocene: A gridded pollen-based reconstruction and its multi-proxy evaluation,  
30 *Quaternary Sci. Rev.*, 112, 109-127, doi:10.1016/j.quascirev.2015.01.013, 2015.

1 Mitchell, L., Brook, E., Lee, J., Buizert, C. and Sowers, T.: Constraints on the late Holocene  
2 anthropogenic contribution to the atmospheric methane budget, *Science*, 342, 964-966.  
3 doi:10.1126/science.1238920, 2013.

4 Oglesby, R. J., Sever, T. L., Saturno, W., Erickson III, D. J. and Srikishen, J.: Collapse of  
5 the Maya: Could deforestation have contributed?, *J. Geophys. Res.*, 115, D12106,  
6 doi:10.1029/2009JD011942, 2010.

7 Peltier, W. R.: Global glacial isostasy and the surface of the ice-age Earth: the ICE-5G (VM2)  
8 model and GRACE, *Annu. Rev. Earth Pl. Sc.*, 32, 111-149,  
9 doi:10.1146/annurev.earth.32.082503.144359, 2004.

10 Petit, J. R., Lipenkov, V. Y., Kotlyakov, V. M., Barkov, N. I., Bender, M., Davis, M.,  
11 Delaygue, G., Barnola, J.-., Stievenard, M., Lorius, C., Delmotte, M., Pepin, L., Chappellaz,  
12 J., Saltzman, E., Legrand, M., Basile, I., Jouzel, J., Raynaud, D. and Ritz, C.: Climate and  
13 atmospheric history of the past 420000 years from the Vostok ice core, *Antarctica, Nature*,  
14 399, 429-436. doi:10.1038/20859, 1999.

15 Piperno, D. R., Ranere, A. J., Holst, I., Iriarte, J., and Dickau, R.: Starch grain and phytolith  
16 evidence for early ninth millennium BP maize from the Central Balsas River Valley,  
17 Mexico, *P. Natl. Acad. Sci.*, 106, 5019-5024, doi: 10.1073/pnas.0812525106, 2009.

18 Pitman, A. J., de Noblet-Ducoudré, N., Cruz, F. T., Davin, E. L., Bonan, G. B., Brovkin, V.,  
19 Claussen, M., Delire, C., Ganzeveld, L., Gayler, V., Hurk, v.d., B. J. J. M., Lawrence, P.J.,  
20 Molen, v.d., M. K., Müller, C., Reick, C.H., Seneviratne, S.I., Strengers, B.J. and Voldoire, A.:  
21 Uncertainties in climate responses to past land cover change: First results from the LUCID  
22 intercomparison study, *Geophys. Res. Lett.*, 36, L14814. doi:10.1029/2009GL039076, 2009.

23 Pongratz, J., Reick, C., Raddatz, T., and Claussen, M.: A reconstruction of global agricultural  
24 areas and land cover for the last millennium, *Global Biogeochem. Cy.*, 22, GB3018.  
25 doi:10.1029/2007GB003153, 2008.

26 Pongratz, J., Reick, C. H., Raddatz, T., and Claussen, M.: Biogeophysical versus  
27 biogeochemical climate response to historical anthropogenic land cover change, *Geophys.*  
28 *Res. Lett.*, 37, L08702, doi:10.1029/2010GL043010, 2010.

29 Pope, V. D., Gallani, M. L., Rowntree, P. R., and Stratton, R. A.: The impact of new physical  
30 parametrizations in the Hadley centre climate model: HadAM3, *Clim. Dynam.*, 16, 123-146.  
31 doi:10.1007/s003820050009, 2000.

1 Roberts, N.: The Holocene: an Environmental History, John Wiley and Sons, 2013.

2 Ruddiman, W. F.: The anthropogenic greenhouse era began thousands of years ago, *Climatic*  
3 *Change*, 61, 261-293. doi:10.1023/B:CLIM.0000004577.17928.fa, 2003.

4 Ruddiman, W. F.: The early anthropogenic hypothesis: Challenges and responses, *Rev.*  
5 *Geophys.*, 45, RG4001. doi:10.1029/2006RG000207, 2007.

6 Ruddiman, W. F.: The Anthropocene, *Annu. Rev. Earth Pl. Sc.*, 41, 45-68.  
7 doi:10.1146/annurev-earth-050212-123944, 2013.

8 Schmidt, G. A., Shindell, D. T., and Harder, S.: A note on the relationship between ice core  
9 methane concentrations and insolation, *Geophys. Res. Lett.*, 31, doi:10.1029/2004GL021083,  
10 2004.

11 [Shepherd, T. G.: Atmospheric circulation as a source of uncertainty in climate change](#)  
12 [projections, \*Nat. Geosci.\*, 7, 703-708. doi:10.1038/NGEO2253, 2014.](#)

13 Singarayer, J. S., and Valdes, P. J.: High-latitude climate sensitivity to ice-sheet forcing over  
14 the last 120kyr. *Quaternary Sci. Rev.*, 29, 43-55. doi:10.1016/j.quascirev.2009.10.011, 2010.

15 Singarayer, J. S., Valdes, P. J., Friedlingstein, P., Nelson, S., and Beerling, D. J.: Late  
16 Holocene methane rise caused by orbitally controlled increase in tropical sources, *Nature*,  
17 470, 82-85. doi:10.1038/nature09739, 2011.

18 Spahni, R., Chappellaz, J., Stocker, T.F., Loulergue, L., Hausammann, G., Kawamura, K.,  
19 Flückiger, J., Schwander, J., Raynaud, D., Masson-Delmotte, V. and Jouzel, J.: Atmospheric  
20 methane and nitrous oxide of the late Pleistocene from Antarctic ice cores, *Science*, 310,  
21 1317-1321. doi:10.1126/science.1120132, 2005.

22 Strandberg, G., Kjellström, E., Poska, A., Wagner, S., Gaillard, M.J., Trondman, A.K., Mauri,  
23 A., Davis, B.A.S., Kaplan, J.O., Birks, H.J.B., Bjune, A.E., Fyfe, R., Giesecke, T., Kalnina,  
24 L., Kangur, M., van der Knaap, W.O. , Kokfelt, U., Kuneš, P., Latalowa, M., Marquer, L.,  
25 Mazier, F., Nielsen, A.B., Smith, B., Seppä, H. and Sugita, S.: Regional climate model  
26 simulations for Europe at 6 and 0.2 k BP: sensitivity to changes in anthropogenic  
27 deforestation, *Clim. Past*, 10, 661-680. doi:10.5194/cp-10-661-2014, 2014.

28 Tauger, M.B: *Agriculture in world history*, Routledge, 2013.

29 Tubi, A., and Dayan, U.: The Siberian high: Teleconnections, extremes and association with  
30 the Icelandic low, *Int. J. of Climatol.*, 33, 1357-1366, doi:10.1002/joc.3517, 2013.

1 [Wanner, H., Beer, J., Bütikofer, J., Crowley, T.J., Cubasch, U., Flückiger, J., Goosse, H.,](#)  
2 [Grosjean, M., Joos, F., Kaplan, J.O., Küttel, M., Müller, S.A., Prentice, I.C., Solomina, O.,](#)  
3 [Stocker, T.F., Tarasov, P., Wagner, M. and Widmann, M.: Mid- to Late Holocene climate](#)  
4 [change: an overview, Quaternary Sci. Rev., 27, 1791-1828,](#)  
5 [doi:10.1016/j.quascirev.2008.06.013, 2008.](#)

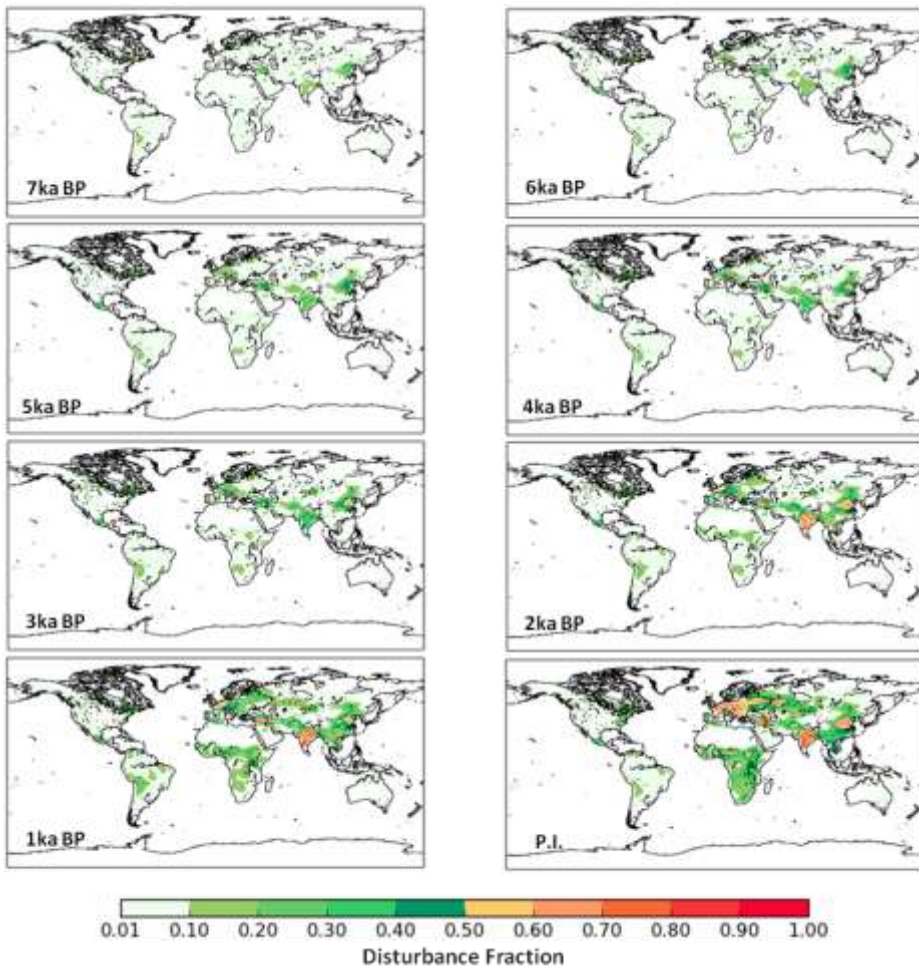
**Formatted:** Font: (Default) Times  
New Roman, 12 pt, Font color: Auto

**Formatted:** Font color: Auto

6 Zohary, D., Hopf, M., and Weiss, E.: Domestication of plants in the old world: The origin and  
7 spread of domesticated plants in south-west Asia, Europe, and the Mediterranean basin, 4th  
8 edn., Oxford University Press, Oxford, 2012.

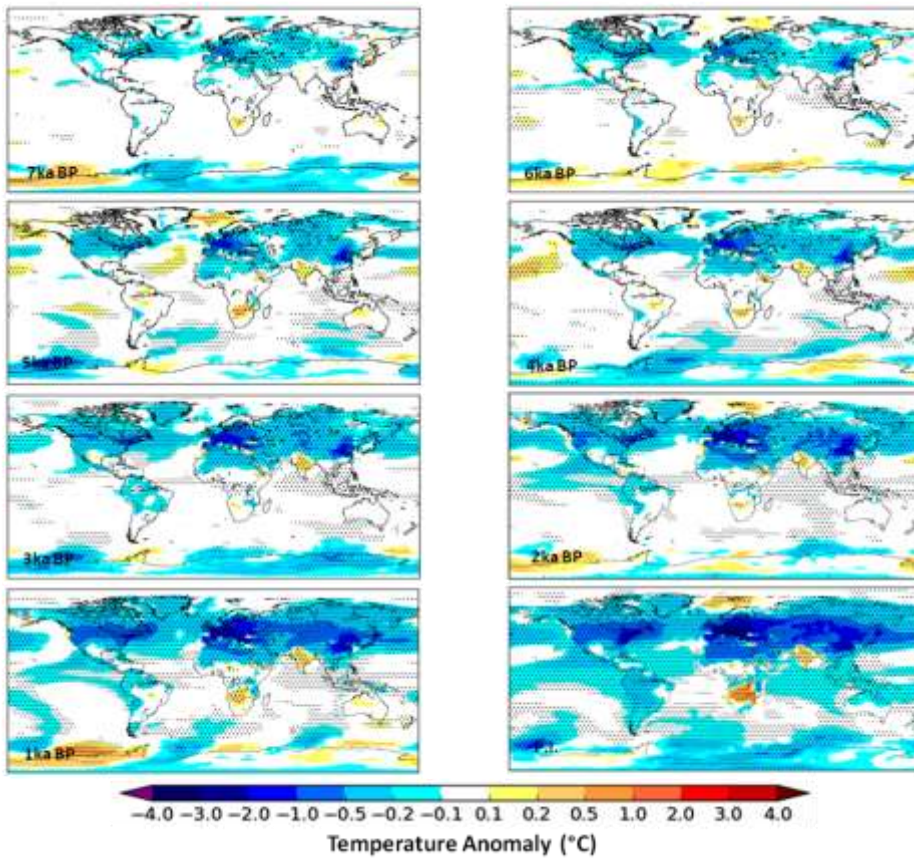
9  
10  
11  
12  
13  
14  
15  
16  
17  
18  
19  
20  
21  
22  
23  
24  
25  
26  
27



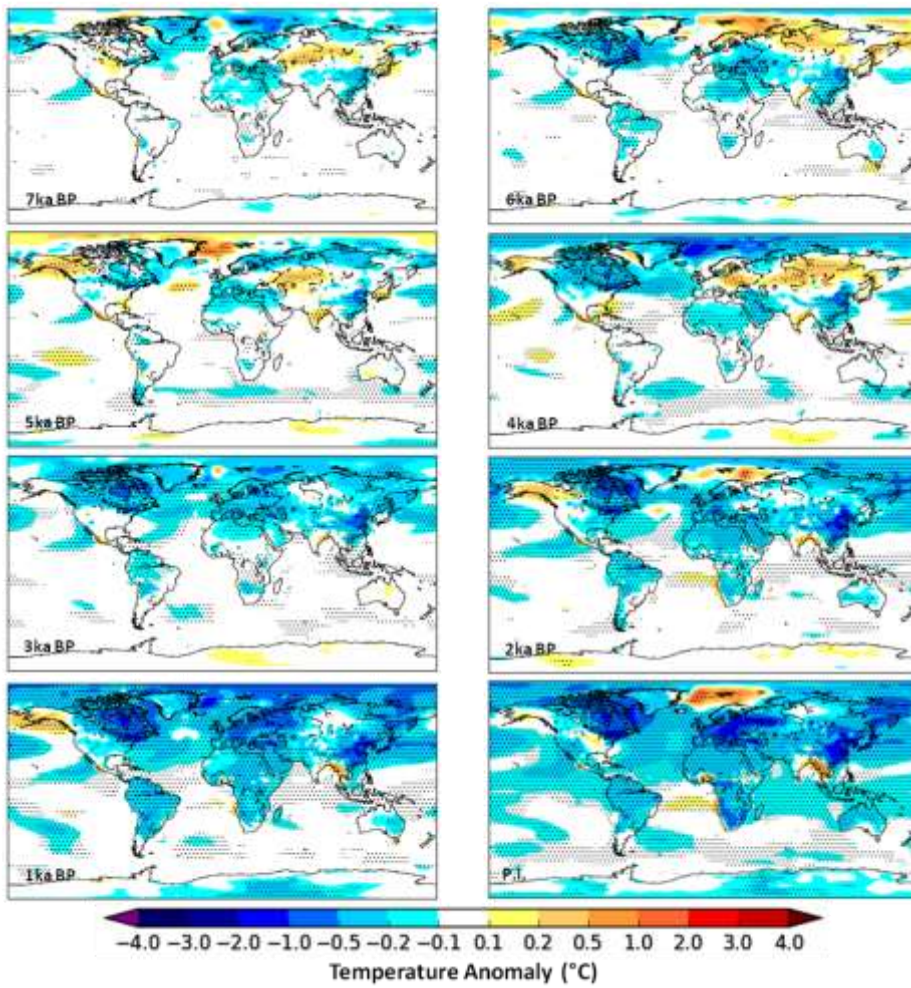


1  
2  
3  
4  
5  
6  
7  
8  
9

**Figure 1.** Fraction of anthropogenically disturbed land at 1000 year intervals from the late pre-industrial (1850 CE) period to 7kaBP. The land disturbance data is based on the anthropogenic land-use scenario KK10 (Kaplan et al., 2009, 2011).



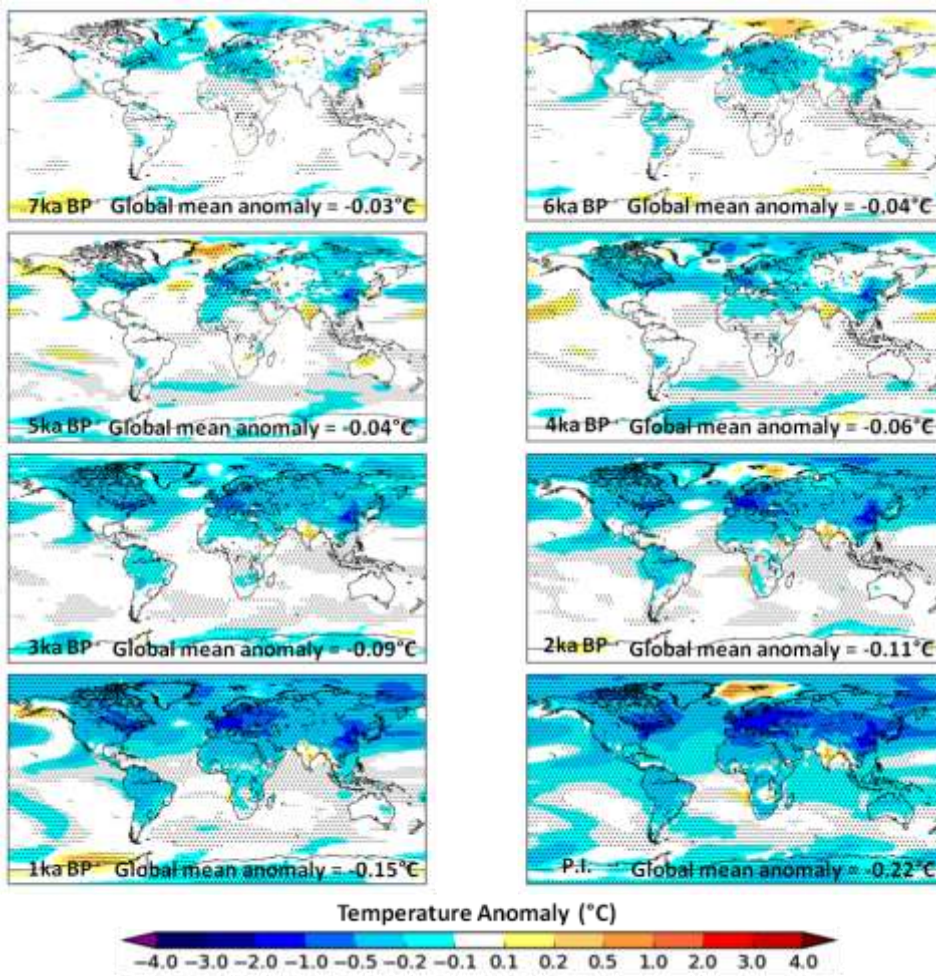
1  
 2  
 3 **Figure 2.** JJA Temperature Anomalies (°C) for KK10 minus Control at timeslices from the  
 4 late pre-industrial period (1850 CE) to 7kaBP. The stippling indicates grid boxes where the  
 5 anomalies are significant at the 95% level using Wilcoxon ranksum statistical analysis.



1  
2  
3 **Figure 3.** DJF Temperature Anomalies (°C) for KK10 minus Control at timeslices from the  
4 late pre-industrial period (1850 CE) to 7kaBP. The stippling indicates grid boxes where the  
5 anomalies are significant at the 95% level using Wilcoxon ranksum statistical analysis.

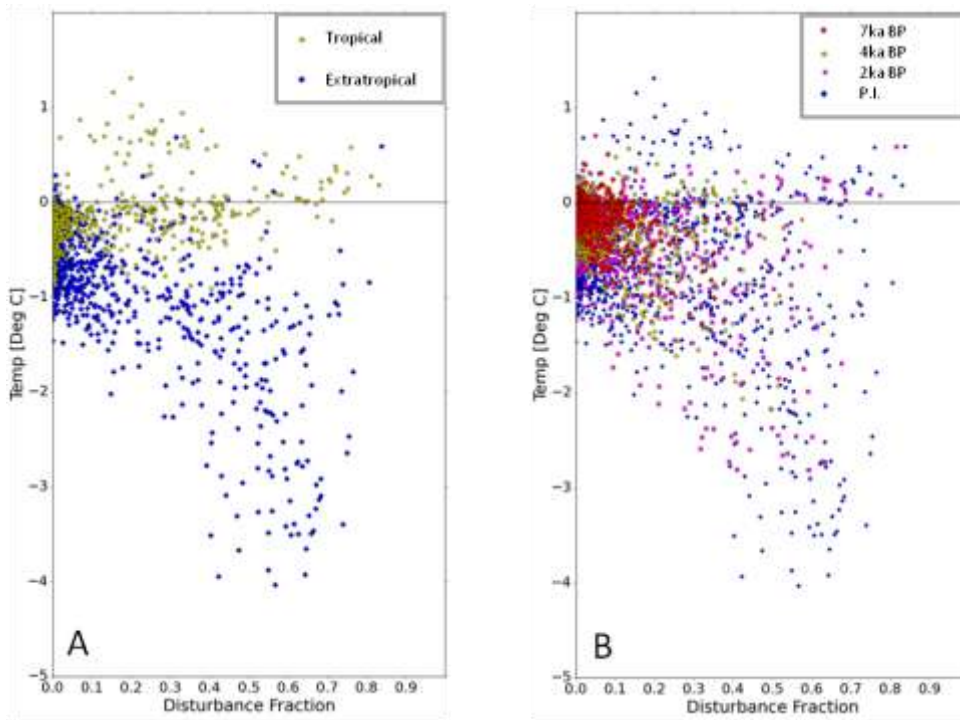
6





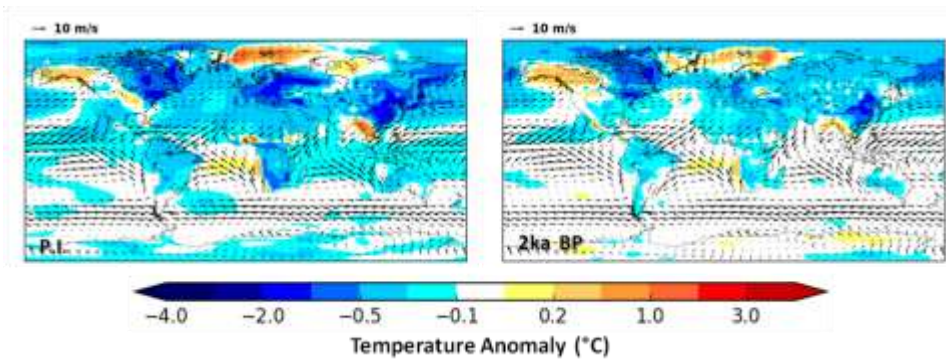
1  
2  
3  
4  
5  
6

**Figure 4.** Annual Temperature Anomalies (°C) for KK10 minus Control at timeslices from the late pre-industrial period (1850 CE) to 7kaBP. The stippling indicates grid boxes where the anomalies are significant at the 95% level using Wilcoxon ranksum statistical analysis.



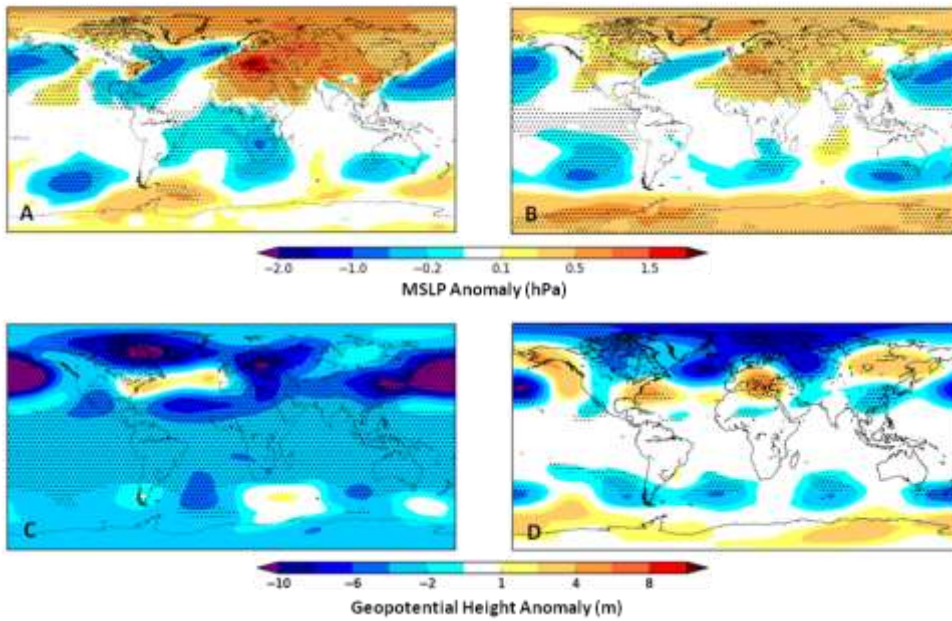
1  
2  
3 **Figure 45.** Relationship between the fraction of anthropogenically disturbed land (from  
4 KK10) and the resultant JJA temperature anomaly (°C). **(a)** For the late pre-industrial (1850  
5 CE) period for extratropical and tropical grid cells. **(b)** For 7kaBP, 4kaBP, 2kaBP and late  
6 pre-industrial (1850 CE) timeslices.

7  
8  
9



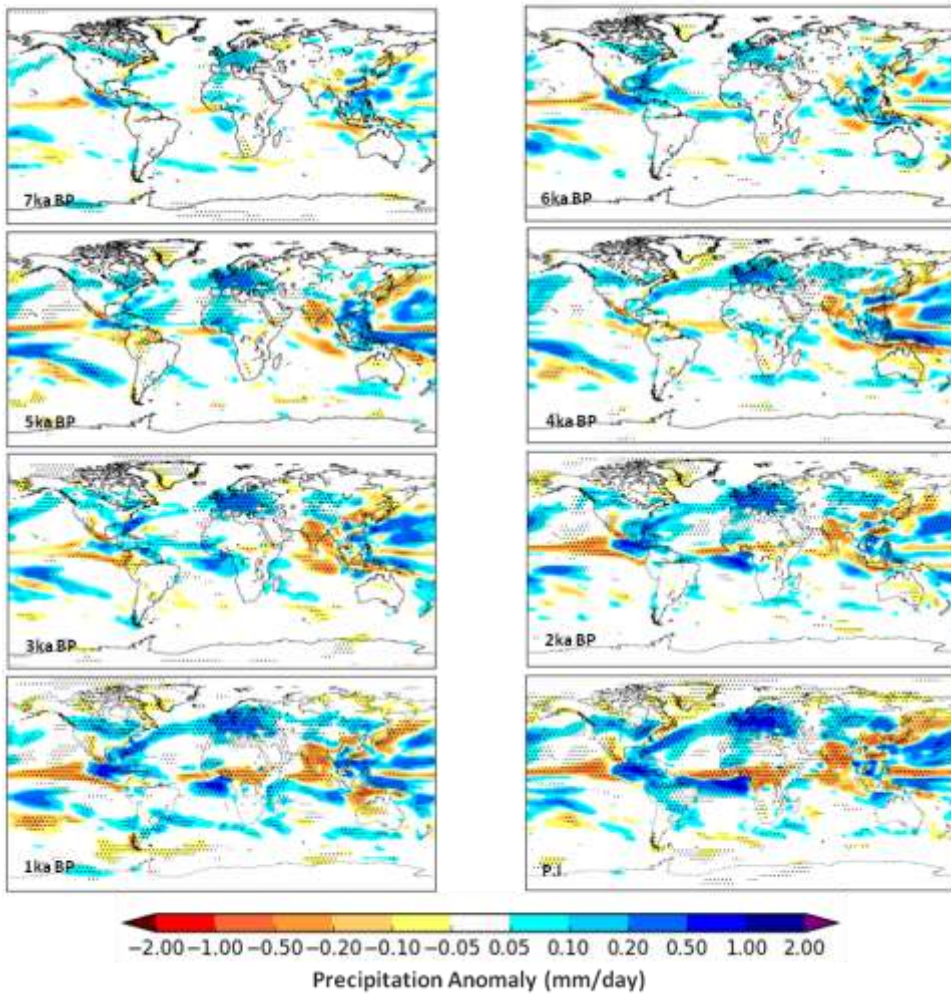
1  
2  
3  
4  
5  
6  
7  
8  
9  
10

**Figure 65.** DJF surface temperature anomalies for KK10 - Control and KK10 surface winds for the late pre-industrial (1850 CE) and 2kaBP.

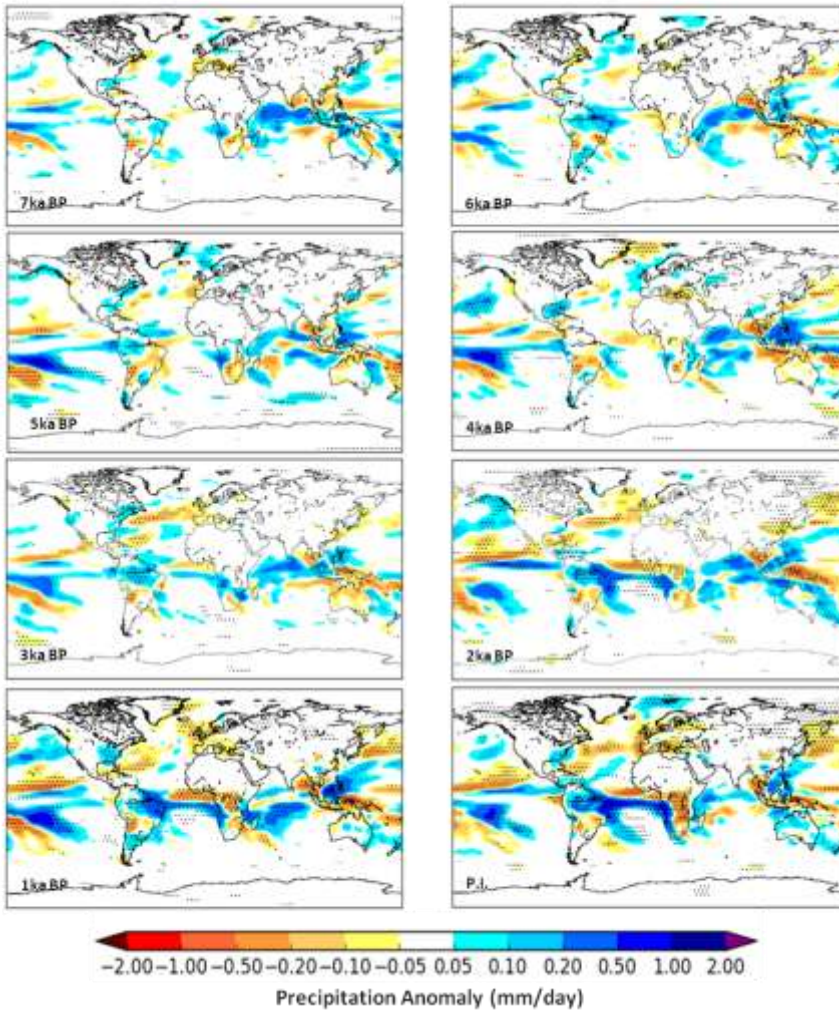


1  
 2  
 3 **Figure 76.** Modifiers of climate in regions outside the areas of anthropogenic land use  
 4 change. All anomalies are for KK10 - Control: (a) JJA MSLP changes at 1850 CE, the  
 5 stippling indicates grid boxes where the anomalies are significant at the 95% level using  
 6 Wilcoxon ranksum statistical analysis; (b) as (a) but for 4kaBP; (c) DJF 500Pa geopotential  
 7 height anomalies at 1850 CE demonstrating stationary wave pattern. The stippling indicates  
 8 grid boxes where the anomalies are significant at the 95% level using Wilcoxon ranksum  
 9 statistical analysis. (d) as (c) but for 4kaBP.

10  
 11  
 12  
 13

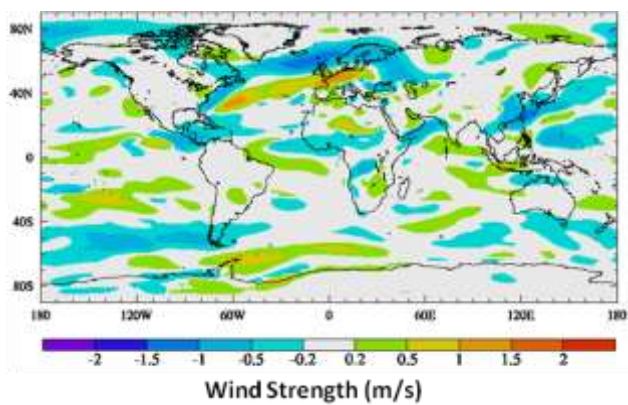


1  
 2  
 3 **Figure 87.** JJA Precipitation Anomalies ( $\text{mm day}^{-1}$ ) for KK10 minus Control at timeslices  
 4 from the late pre-industrial period (1850 CE) to 7kaBP. The stippling indicates grid boxes  
 5 where the anomalies are significant at the 95% level using Wilcoxon ranksum statistical  
 6 analysis.



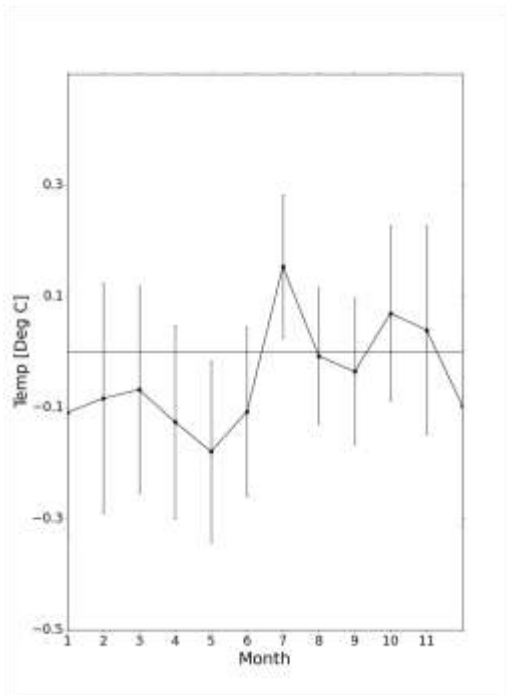
1  
2  
3  
4  
5  
6  
7  
8

**Figure 89.** DJF Precipitation Anomalies ( $\text{mm day}^{-1}$ ) for KK10 minus Control at timeslices from the late pre-industrial period (1850 CE) to 7kaBP. The stippling indicates grid boxes where the anomalies are significant at the 95% level using Wilcoxon ranksum statistical analysis.



1  
2  
3 | **Figure 910.** JJA 850hPa Wind Strength Anomalies ( $\text{ms}^{-1}$ ) for KK10 minus Control for the  
4 late pre-industrial period (1850).

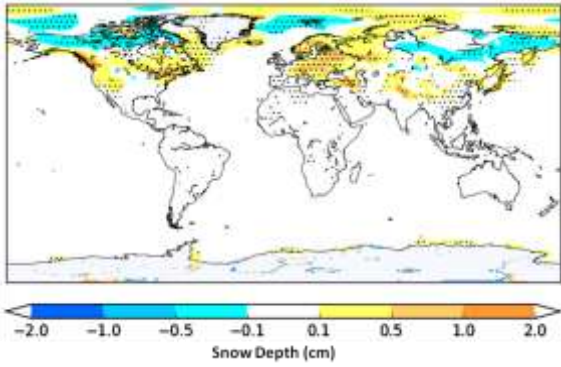
5  
6  
7  
8



1  
2  
3  
4  
5  
6  
7  
8  
9

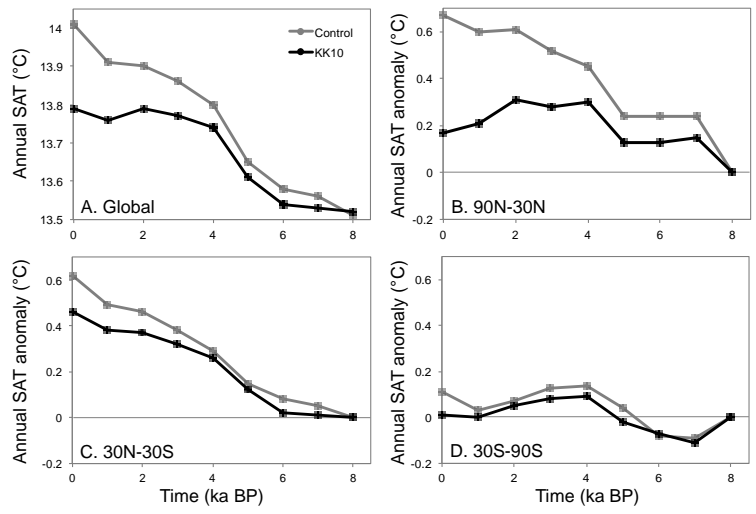
**Figure 1011.** Indian temperature seasonality; KK10 - Control surface temperature anomalies for the late pre-industrial (1850CE) simulation; the vertical bars indicate the normal range of variability which is considered to be within 2 standard deviations of the mean.





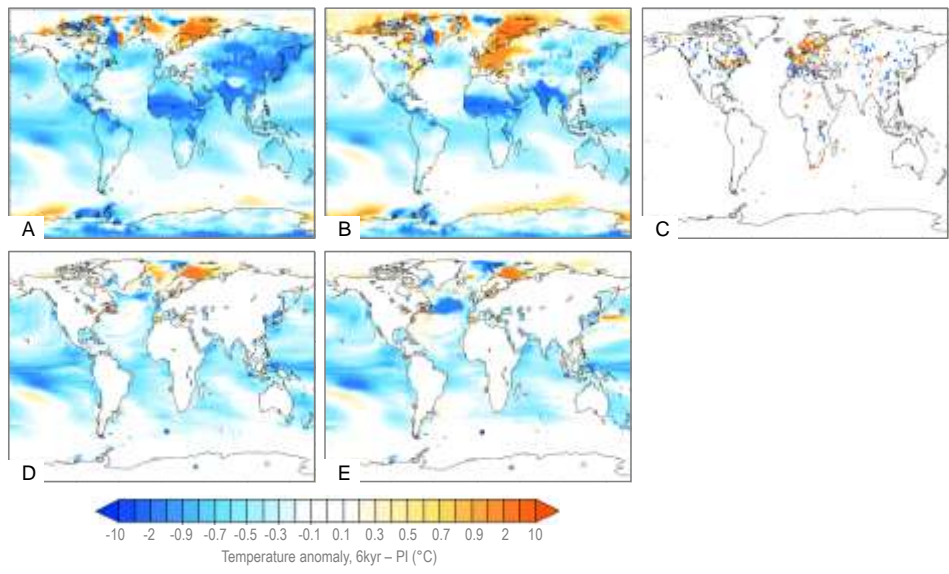
1  
2

3 | **Figure 4.12.** DJF Snowdepth Anomalies (cm) for KK10 minus Control for the late pre-  
4 industrial period (1850 CE). The stippling indicates grid boxes where the anomalies are  
5 significant at the 95% level using Wilcoxon ranksum statistical analysis.



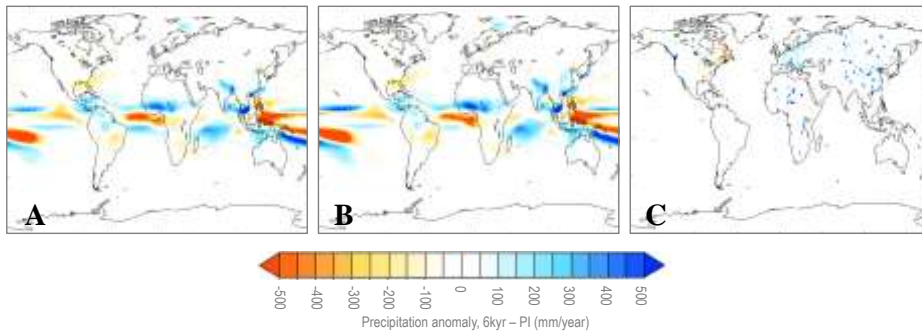
1  
2 **Figure 1213.** Time series plots for the Holocene simulations from HadCM3. **(a)** annual mean  
3 global Surface Air Temperature (SAT) for the Control simulation in grey, and KK10  
4 simulation in black; **(b)** anomaly in northern extratropical (30-90N) annual mean temperature  
5 from the equivalent simulation at 8kaBP; **(c)** same as **(b)** but for the tropics (30N-30S); **(d)**  
6 same as **(b)** but for the southern extratropics (30-90S).

7  
8  
9  
10  
11



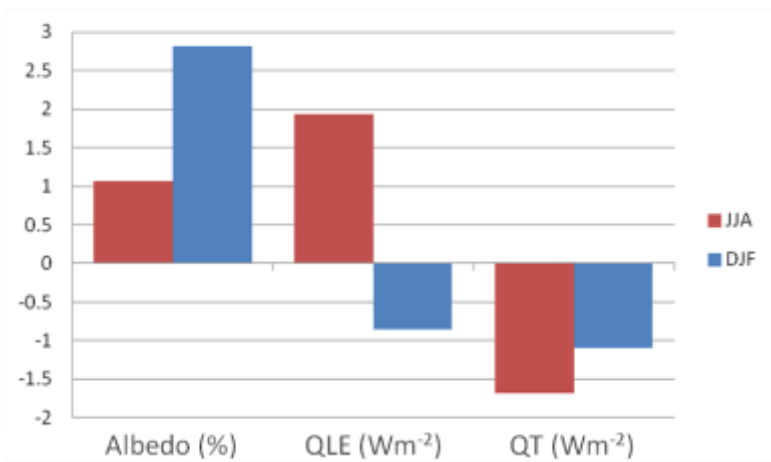
1  
2 **Figure 1314.** Mid-Holocene minus Pre-Industrial temperature anomalies. **(a)** annual mean  
3 surface air temperature anomalies from the control experiment; **(b)** annual mean surface air  
4 temperature anomalies from the KK10 experiment; **(c)** Bartlein et al. (2011) pollen-based  
5 reconstructions of the mean annual air temperature anomaly; **(d)** ocean annual mean  
6 temperature for the top two layers (25m) from the control experiment with palaeo-proxy  
7 reconstructions (Marcott et al., 2013) overlain in coloured circles ; **(e)** as in **(d)** but for the  
8 KK10 experiment.

9  
10  
11  
12

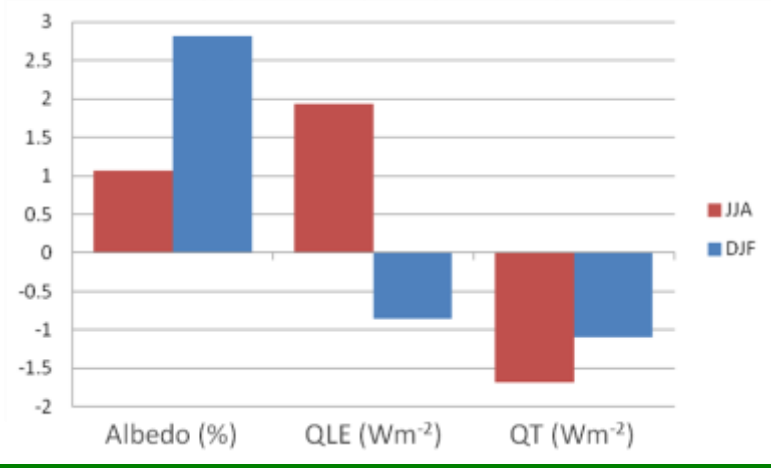


1  
2 **Figure 1415.** Mid-Holocene minus Pre-Industrial precipitation anomalies. **(a)** annual mean  
3 precipitation anomalies from the control experiment; **(b)** annual precipitation anomalies from  
4 the KK10 experiment; **(c)** Bartlein et al. (2011) pollen-based reconstructions of the mean  
5 annual precipitation anomaly.

6  
7  
8  
9  
10  
11  
12  
13  
14



1



2

3

4

5

6

7

8

9

**Figure 16.** JJA and DJF albedo, latent heat flux (QLE) and turbulent heat flux (QT) anomalies for KK10 minus Control for the late pre-industrial period (1850 CE) for the North America/Eurasia land surface.

1 **Authors' Response**

2

3 **Response to Anonymous Reviewer #1**

4 Thank you very much for taking the time and trouble to review our manuscript and for your  
5 helpful comments and suggested references. Our responses to your comments/queries are as  
6 follows:

7 COMMENT: Abstract Maybe the authors already can add some numbers how large global  
8 and regional changes are in degrees centigrade – it's trivial to achieve a statistically  
9 significant result when the number of samples is high enough. The physical significance  
10 might however be irrelevant then.

11 RESPONSE: Global mean temperature changes and maximum regional change (Europe) for  
12 7ka BP, 2ka BP and PI have been added to the abstract. The comment on statistical  
13 significance is addressed below in response to the comments on section 2.1.

14 COMMENT: 1 Introduction The introduction lacks a general presentation of forcings  
15 potentially influencing Holocene climate such as orbital, solar, volcanic and GHG (for an  
16 overview refer e.g. Schmidt et al. 2011) – in the present form the reader who is not too  
17 familiar with the topic might get the impression that only changes in land use were the main  
18 driver of Holocene climatic changes

19 RESPONSE: A brief description of the natural forcings has been added to the introduction.

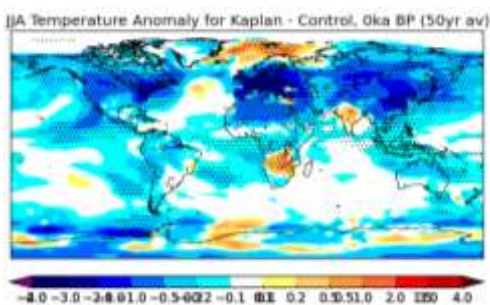
20 COMMENT: 2.1 Model description: The authors state the model does not include an  
21 interactive carbon module – which effect might the change in land use have on the carbon  
22 cycle ? In their introduction they note that besides the biogeophysical effects there are also  
23 biogeochemical effects in terms of changes in CO<sub>2</sub> that might offset parts of the albedo  
24 changes induced by land use changes.

25 RESPONSE: Anthropogenic land use changes normally involve deforestation thus reducing  
26 the vegetation carbon sink and releasing carbon to the atmosphere particularly if slash and  
27 burn agriculture is practised resulting in little carbon being stored in the soil. Kaplan et al  
28 (2010) estimated that by AD 1850 cumulative carbon emissions due to land use changes were  
29 325–357 Pg. Some of this excess CO<sub>2</sub> will be absorbed by the oceans but much will remain in  
30 the atmosphere and, as a greenhouse gas, it will contribute to an increase in global

1 temperatures. The lack of an interactive carbon module in our model means that these  
2 atmospheric CO2 changes and resultant warming are not included in our results.

3 COMMENT: In the last paragraph of the section authors state that changes in land use are  
4 very small and localized and therefore one needs to integrate very long times to find a small  
5 albeit statistically significant result – I find this strategy a bit unfavorable because a priori this  
6 will most likely result in a statistically significant difference independent to the physical  
7 significance of the signal (see also von Storch and Zwiers, 1999).

8 RESPONSE: As climate data demonstrates variability on a range of timescales it was felt that  
9 a longer averaging period would encompass as many modes of variability as possible and thus  
10 give a more robust result. There is the potential to get the wrong results if short averaging  
11 periods are used. There were effectively 500 samples in our statistical analysis which, for  
12 temperature, gives an effect size of about 0.1°C, the minimum contour level used in our plots.  
13 Whilst a small difference, its inclusion does add value to the contour plots as it helps visualise  
14 the patterns of anomalies in the contour plots and thus to understand the dynamics of the  
15 climatic changes. It is worth noting that when the test is run with 50 samples (Figure 1) the  
16 results over the major land masses were still found to be statistically significant.



17  
18 Figure 1: JJA Temperature Anomalies (°C) for KK10 minus Control for the late pre-industrial period (1850 CE)  
19 averaged over a 50 year period. The stippling indicates grid boxes where the anomalies are significant at the  
20 95% level using Wilcoxon ranksum statistical analysis.

21 COMMENT: 3 Results Given the effect of changes in RF due to changes in land use,  
22 especially in the earlier periods, temperature changes seem to be quite large – According to  
23 Fig. 2, the change amounts to 2-3 K in the pre-industrial period over parts of Europe and  
24 North America. The temperature increase over these regions is approximately 1-1.5 K in the  
25 last 150 years (cf. Supplement of PAGES2k reconstructions). Given this strong impact of land  
26 use changes, the temperatures should even decrease over these regions due to the presence of  
27 the land use changes. Earlier modelling studies with constant land cover also show

1 temperature evolutions that are comparable to proxy reconstructions using only changes in  
2 solar, volcanic and GHG concentrations – how do the authors explain such large impact of  
3 land use change?

4 RESPONSE: The cooling effect of the biogeophysical impacts of ALCC is countered by the  
5 biogeochemical effects (increased methane and CO<sub>2</sub> production) which increase  
6 temperatures. On a global average scale and in most individual regions the overall effect of  
7 ALCC when both physical and chemical effects are taken into account the net result will be a  
8 warming. As previously mentioned the lack of an interactive carbon module in our model  
9 means that we are unable to quantify these atmospheric CO<sub>2</sub> changes. However, in a similar  
10 study that also included the biogeochemical changes, He et al, 2014 estimated that by 1850  
11 CE the biogeophysical feedbacks of Holocene ALCC caused a global cooling of 0.17°C,  
12 while biogeochemical feedbacks caused a 0.90°C global warming i.e. the biogeochemical  
13 effects of land use were a factor of 5 more important than the biogeophysical effects on the  
14 global scale and the physical effects are only dominant in the regions of greatest ALCC such  
15 as Europe, N.E. America & E. Asia. In addition during the last 150 years there has been a big  
16 increase in greenhouse gas emissions from industrial sources. The cumulative CO<sub>2</sub> &  
17 methane emissions from industrial sources between 1750 and 2010 have been about 4 times  
18 the magnitude of those from land use (IPCC, AR5, SPM, 2014). These industrial emissions  
19 would further serve to counter the cooling due to the biogeophysical impacts of land use  
20 change. Other considerations are uncertainties in the land use reconstructions. Using the  
21 HYDE 3.1 data resulted in smaller anomalies although we feel that the KK10 data is probably  
22 more realistic for the reasons outlined in Section 5 (Discussion) of the manuscript. Also, as  
23 mentioned later, the equilibrium response could be different to the response achieved when  
24 using a transient simulation. The inclusion of ALCC improved the data-model comparison for  
25 HadCM3. For a discussion of the relative merits of HadCM3 please see the following  
26 response and the response to comments on Section 4.

27 COMMENT: Another important point relates to the treatment of convection, soil moisture  
28 and hence cloud cover – the drying of soils would eventually lead to less convection and less  
29 cloud cover leading to increase in shortwave radiation counteracting the increase in albedo  
30 due to land cover change. How well does HadCM3 address these processes that would be  
31 important to assess the full range and implications of land use changes, especially on the local  
32 scale ?



1 RESPONSE: Soil moisture and the exchange of moisture between the surface and the  
2 atmosphere is calculated by MOSES II (Met Office Surface Exchange Scheme) which is  
3 coupled to HadCM3. In MOSES soil moisture is represented on four subsurface layers. The  
4 soil moisture is treated as homogeneous across a grid box. Bare-soil evaporation is drawn  
5 from the surface soil layer only. Harris et al (2004) found that MOSES/HadCM3 was able to  
6 simulate the observed fluxes of heat, moisture and carbon in Amazonia with reasonable  
7 accuracy. HadCM3 uses the penetrative convective scheme (Gregory and Rowntree 1990)  
8 modified to include an explicit downdraught and the direct impact of convection on  
9 momentum (Gregory et al. 1997). The large-scale precipitation and cloud scheme is  
10 formulated in terms of an explicit cloud water variable (Smith, 1990). Johns et al (2003)  
11 found that generally HadCM3 is effective at capturing the patterns of mean seasonal  
12 precipitation for DJF and JJA when judged against the CMAP (CPC Merged Analysis of  
13 Precipitation) climatology (Xie and Arkin 1997). The agreement over land, where the  
14 climatology is more reliable, was particularly good, giving confidence in the model physics.  
15 HadCM3 does however overestimate the precipitation in the eastern tropical Atlantic and the  
16 Gulf of Guinea. In general, HadCM3 ranked highly in CMIP 2 & 3 over a range of climate  
17 variables compared to other models (Reichler and Kim (2008) compared an aggregate score  
18 for 14 climate variables) and it was one of the major models used in the IPCC Third and  
19 Fourth Assessments and contributed to the Fifth Assessment.

20 COMMENT: How do results quantitatively compare to other studies (e.g. Pongratz et al. 2010  
21 and Betts et al. 2007, Brovkin et al. 2004) suggesting considerable less impact of changes in  
22 land use change on regional and global temperatures. Might therefore part of the results be a  
23 specific model-dependent issue ?

24 RESPONSE: In the discussion (Section 5) we compare our results to those from He et al,  
25 2014 and Pongratz et al 2010. We found similarities in the distribution of the temperature  
26 anomalies with those found by He et al (2014) for 1850 CE and Pongratz et al (2010) for the  
27 20th century although the temperature changes found in this study were greater e.g. a pre-  
28 industrial global annual mean temperature anomaly of  $-0.23^{\circ}\text{C}$  as opposed to the  $-0.17^{\circ}\text{C}$   
29 estimated by He et al (2014). Not all the other studies use comparable time slices and so a  
30 direct quantitative comparison is not always possible.

31 COMMENT: Please also consult the study of Boisier et al. 2012 for a more thorough  
32 discussion of potential effects of changes in other properties related to changes in land use

1 and the dependence on specific model and model configuration. An example for a time slice,  
2 preferably the PI vs present day concerning a separation into different components (albedo,  
3 latent and turbulent heat fluxes) as carried out in the study of Boisier et al. 2012 would also  
4 help to assess the model-specific response on land use changes.

5 RESPONSE: Figure 16 has been added which shows the KK10 - Control albedo, latent and  
6 turbulent heat flux changes for PI.

7 COMMENT: 3.1.2 Remote impacts of land use I wonder why the authors did not carry out in  
8 parallel a transient simulation with continuous changes in land use including changes in  
9 orbital parameters – The reason is that the equilibrium response could be different to the  
10 response one achieves when using a transient simulation – although this kind of simulation  
11 would lie outside the scope of the present manuscript at least some words addressing potential  
12 implications would be helpful to put results obtained with the multi-centennial long-time slice  
13 experiments into perspective.

14 RESPONSE: We agree that it would be very interesting to run a transient simulation but it  
15 was not practical to do so within the already wide scope of this manuscript. We are building  
16 on snap-shot simulations that are previously published for the last glacial cycle (Singarayer  
17 and Valdes, 2010; Singarayer et al., 2011) and these land-use time slices expand our work  
18 using this methodology. In addition, with the speed of the model and HPC queuing times it  
19 would have taken more than two years to complete a Holocene transient simulation and so  
20 was not possible within this particular project time frame, although we would very much like  
21 to be able to do this in future. We had mentioned the advantages of running a transient  
22 simulation within the discussion but have added more emphasis to that statement.

23 COMMENT: 3.2 Atmospheric dynamics How can low-level surface winds advect changes  
24 into remote regions ? I would rather expect a mid-to-high altitude mechanism driving low  
25 levels wind. Also the still coarse resolution of the global climate model will not properly  
26 simulate a realistic pattern of low-level winds, especially over regions characterized by a  
27 complex land-sea mask and regions with complex topography.

28 RESPONSE: As suggested below the order of the sections has been changed and the  
29 renumbered section 3.2.3 has been rephrased to state that the surface winds will advect  
30 changes into adjacent (rather than remote) regions. We agree that in most regions there won't  
31 be a recognisable or predictable pattern of advection but where there is a prevailing wind  
32 direction advection of temperature anomalies can be seen.

1 COMMENT: 3.2.2 Mean sea level pressure I suggest to change the order of the sections  
2 starting with upper tropospheric dynamics, to mslp and eventually low-level dynamics.  
3 Changes in mslp will change the surface wind pattern In general I have some reservations  
4 with the purely thermal explanations of wind changes in the extratropics excluding dynamical  
5 reasoning for instance related to changes in baroclinicity due to changes in the overall  
6 meridional temperature gradient also affecting the uppertropospheric circulation

7 RESPONSE: The order of the sections has been changed and the renumbered section 3.2.1  
8 includes dynamical reasoning as suggested.

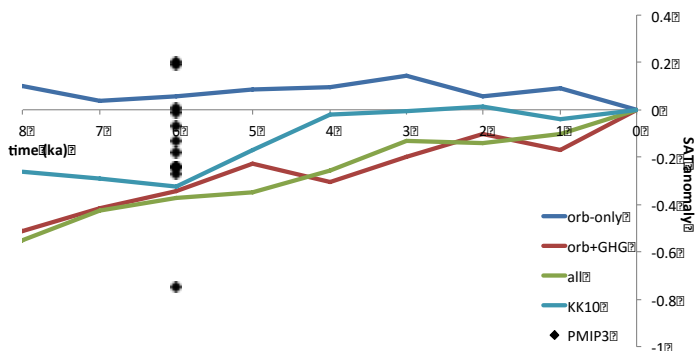
9 COMMENT: 3.3 Hydroclimate Analyzing hydroclimate changes from GCM output is  
10 afflicted with high uncertainties – this should be noted somewhere because results based on  
11 only one model can lead to false or not robust conclusions given the high degree of  
12 uncertainty even the current generation of GCM/ESM shows for the hydrological cycle.

13 RESPONSE: We agree that there are uncertainties in hydroclimate analysis by GCMs. This  
14 has now been noted in section 3.3 and the discussion. Some aspects such as the movement of  
15 the ITCZ away from a cooling hemisphere are reasonably robust and are seen in other studies  
16 (e.g. Kang et al, 2008).

17 COMMENT: 4 Temporal evolution of Holocene climate Can you explain why especially the  
18 NH temperatures show such a strong temperature increase – the summer insolation decreases  
19 and winter insolation north of 30 °N has not a pronounced effect. Most reconstructions and  
20 simulations point to a decrease in NH temperatures during the Holocene (cf. also Wanner et  
21 al. 2008).

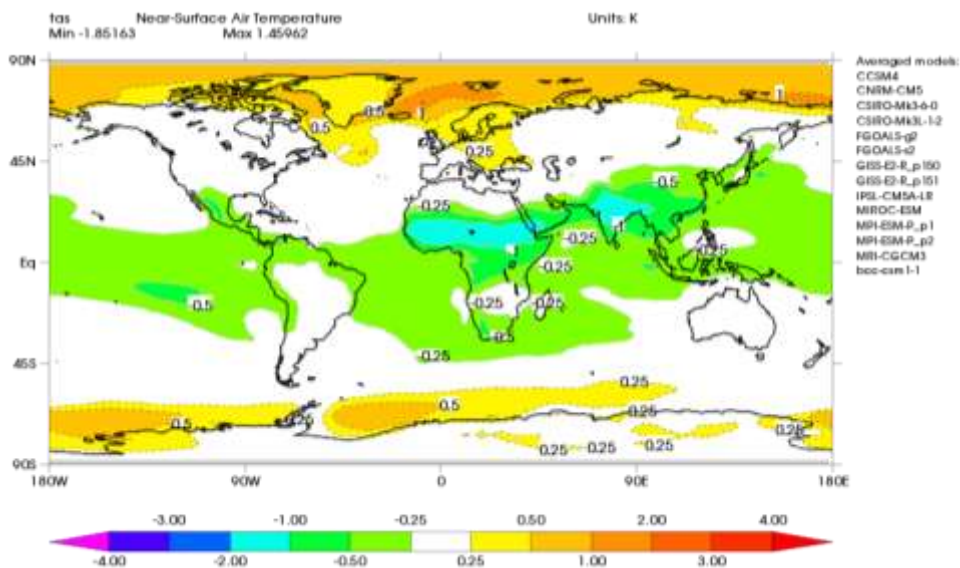
22 RESPONSE: We have previously done sensitivity experiments where the model has been  
23 forced solely with orbital configuration changes, then with greenhouse gas (GHG) variations  
24 in addition, and then with ice-sheet and sea level changes (e.g. Singarayer et al., 2011). In  
25 HadCM3, the simulations with orbit-only variations produce a slight temperature decrease  
26 through the Holocene for the northern hemisphere (30-90N). The cooling from mid-Holocene  
27 to pre-industrial is largest over the Arctic region. The impact of including increasing  
28 greenhouse gases on temperature outweighs the orbital influence and results in an overall  
29 warming over 30-90N. There are still regions over the Arctic and north Atlantic where the  
30 cooling remains, however. Seasonally, we find that cooling through the Holocene still occurs  
31 in northern hemisphere summer, when forced with orbit and GHG variations, but is not as  
32 pronounced as when only forced by orbital variations. In winter, when HadCM3 is forced

1 with orbit-only variation there is little change in temperature, but when GHG increases are  
 2 included this becomes a warming through the Holocene, which then outweighs the reduced  
 3 summer cooling. While the annual mean warming signal is in apparent disagreement with  
 4 some of the palaeodata records, including the recent Marcott et al (2013) record, it is within  
 5 the range of other climate model responses when compared with the PMIP3 (Paleoclimate  
 6 Model Intercomparison Project) model mid-Holocene to pre-industrial temperature  
 7 anomalies. Figure 2 is a plot of the available PMIP3 model global annual mean temperature  
 8 anomalies for mid-Holocene with our HadCM3 time slices for the Holocene. 11 of 13 PMIP3  
 9 models demonstrate little change or warming from 6ka to 0ka, rather than cooling. HadCM3  
 10 has a relatively large warming, although not the largest of all the models. The warming in our  
 11 version of HadCM3 is amplified by the coupled vegetation scheme (which the majority of the  
 12 PMIP3 models still do not include). The increase in modelled forest cover through the  
 13 Holocene, facilitated by CO<sub>2</sub> increase in terms of favourable climate as well as CO<sub>2</sub>  
 14 fertilization, decreases albedo and increases temperatures further.



15  
 16 **Figure 2**

17 When the multi-model mean temperature anomaly map is plotted (Figure 3; taken from the  
 18 PMIP3 website for expediency), the same pattern as for HadCM3 is observed in that the mid-  
 19 Holocene is warmer than pre-industrial over the Arctic, with little change or cooler  
 20 temperatures over mid- and low latitude land, similar to the HadCM3 spatial pattern.



1  
2 **Figure 3**  
3 Palaeodata syntheses such as Bartlein et al (2013), as shown in our paper Figure 13, display  
4 regionally variable mid-Holocene temperature anomalies. There are a number of points over  
5 Eurasia, central N America, and the Mediterranean where their data suggest a regionally  
6 cooler mid-Holocene, while Scandinavia, eastern N America, and some Arctic regions are  
7 inferred to have a warmer mid-Holocene. This is similar to the discussion section of Wanner  
8 et al. (2008, section 6.1), and their figure 18, where the cooling is most evident over the N  
9 Atlantic and higher latitude northern hemisphere, and in some cases is thought to be mainly in  
10 summer. In summary, in HadCM3 the temperature response to increasing Holocene GHGs is  
11 larger than the seasonal decrease in temperatures resulting from decline in summer insolation.  
12 This overall response is not unusual when compared to other PMIP models. There are  
13 regional variations in the response of models with a tendency for cooling at high latitudes but  
14 warming at lower latitudes. While palaeodata syntheses may suggest a cooling of northern  
15 hemisphere temperatures, there also appear to be regional and seasonal variations in the data.  
16 The temperature anomalies are fairly small in both models and data and in addition, with a  
17 lack of data in some areas (particularly outside Europe), there is perhaps significant  
18 uncertainty in both models and data as to what the average northern hemisphere annual mean  
19 temperature response is. We will add a small discussion to the text about why we get a strong  
20 temperature increase in the model and discuss our comparison with data and other models in  
21 section 4.

1 COMMENT: 5 Discussion In general I liked the discussion section as useful to put results  
2 into perspective – However, I don't know if it's wise to criticize studies addressing results for  
3 regional climate change based on a regional climate model, when the GCM of the present  
4 study shows potential shortcomings, i.e. the overall temperature change between MHPI is at  
5 odds with many other studies, the biogeochemical effect and the overall coarse resolution of  
6 the HadCM3 model neglecting specific regional details.

7 RESPONSE: We did not intend our text to read as a criticism of regional models and accept  
8 that no model including HadCM3 is without shortcomings. We have tried to stress that our  
9 results are the results from only one model. For the land use change scenario however we did  
10 feel that it was necessary to point out that an additional issue for regional models would be  
11 that the remote atmospheric changes would not be included. Although the advantages of  
12 regional models might outweigh this disadvantage we believe that this knowledge of these  
13 remote influences could be helpful for others planning model studies in the future. We have  
14 however make the comment more general and also mentioned the advantages of regional  
15 models such as higher resolution.

16 COMMENT: p 4603, l 12. Why is the abbreviation anthropogenic land use change “ALCC”  
17 rather than “ALUC” ?

18 RESPONSE: Anthropogenic land use change has been changed to anthropogenic land cover  
19 change.

20 COMMENT: Section 2.2.: I suggest including a table where the experimental setup is  
21 summarized with according abbreviations.

22 RESPONSE: Table 1 has been added.

23 COMMENT: p 4612 l 24: the weblinks should be replaced by citations from the peer-  
24 reviewed literature

25 RESPONSE: This has been done.

26 COMMENT: In Figure 2 and 3 it would be helpful to include the global average of the  
27 temperature change and also reproduce changes in the annual mean

28 RESPONSE: Figure 4 has been added which reproduces the annual mean anomalies and  
29 includes the global average temperature change.

30 REFERENCES:

1 Gregory, D., & Rowntree, P. R. (1990). A mass flux convection scheme with representation  
2 of cloud ensemble characteristics and stability-dependent closure. *Monthly Weather Review*,  
3 118(7), 1483-1506. doi:10.1175/1520-0493(1990)118<1483:CO;2

4 GREGORY, D., KERSHAW, R., & INNESS, P. (1997). Parametrization of momentum  
5 transport by convection. II: Tests in single-column and general circulation models. *Quarterly*  
6 *Journal of the Royal Meteorological Society*, 123(541), 1153-1183. doi:10.1256/smsqj.54102

7 Harris, P. P., Huntingford, C., Gash, J. H. C., Hodnett, M. G., Cox, P. M., Malhi, Y., &  
8 Araújo, A. C. (2004). Calibration of a land-surface model using data from primary forest sites  
9 in amazonia. *Theoretical and Applied Climatology*, 78(1), 27-45. doi:10.1007/s00704-004-  
10 0042-y

11 Johns, T. C., Gregory, J. M., Ingram, W. J., Johnson, C. E., Jones, A., Lowe, J. A., .  
12 Woodage, M. J. (2003). Anthropogenic climate change for 1860 to 2100 simulated with the  
13 HadCM3 model under updated emissions scenarios. *Climate Dynamics*, 20(6), 583-612.  
14 doi:10.1007/s00382-002-0296-y

15 Reichler, T., & Kim, J. (2008). How well do coupled models simulate today's climate?  
16 *Bulletin of the American Meteorological Society*, 89(3), 303-311. doi:10.1175/BAMS-89-3-  
17 303

18 Smith, R. N. B. (1990). A scheme for predicting layer clouds and their water content in a  
19 general circulation model. *Quarterly Journal of the Royal Meteorological Society*, 116(492),  
20 435-460. doi:10.1002/qj.49711649210

21 Wanner, H., Solomina, O., Grosjean, M., Ritz, S. P., & Jetel, M. (2011). Structure and origin  
22 of holocene cold events. *Quaternary Science Reviews*, 30(21), 3109-3123.  
23 doi:10.1016/j.quascirev.2011.07.010

24 Xie, P., & Arkin, P. A. (1997). Global precipitation: A 17-year monthly analysis based on  
25 gauge observations, satellite estimates, and numerical model outputs. *Bulletin of the*  
26 *American Meteorological Society*, 78(11), 2539-2558. doi:10.1175/1520-  
27 0477(1997)078<2539:CO;2

## 28 **Response to Anonymous Reviewer #2**

29

1 Thank you very much for taking the time and trouble to review our manuscript and for your  
2 helpful comments.

3 COMMENT: Page 4619, Line 20-25. The authors acknowledge that there is a lot of  
4 uncertainty in global land use reconstructions (e.g. HYDE 3.1 is much lower than KK10).  
5 Strangely, ‘The decision was taken to proceed with the KK10 data due to its assumptions of a  
6 larger per capita land use earlier in the Holocene.’ (page 4620, line 1-5). Why is that? Is more  
7 land use per capita better? Better than what? Would the results be different with HYDE?  
8 Please explain.

9 RESPONSE: Early agriculture was much less efficient than agriculture today with tracts of  
10 land left fallow for years. It is estimated that per capita land use for agriculture during the  
11 industrial age is about 0.2-0.3 ha per person (Williams (1990), Grubler (1994)) but was more  
12 like 3ha per person in Neolithic times (e.g. Gregg, 1988). There have been many  
13 technological advances since the advent of agriculture from selective breeding of crops and  
14 animals to fertilisers and more efficient tools. KK10 makes some allowance for these  
15 technological changes and therefore allocates more agricultural land to feed each head of  
16 population earlier in the Holocene than it does in the early industrial period. This we believe  
17 is probably more realistic than constant per capita land use although of course there are still  
18 uncertainties in the data. With the Hyde data the land use changes are less than with KK10  
19 particularly in the earlier time slices. The same pattern of climate change is seen but later and  
20 on a reduced scale.

21 The comment in the discussion has been expanded to make it clearer.

22 COMMENT: Abstract, line 4. ‘Various studies . . .’ needs a reference.

23 RESPONSE: References have added to the abstract.

24

## 25 **List of Major Changes**

26

27 Note:

- 28 • Page/line numbers refer to change tracked version.
- 29 • Figure numbers have been updated throughout.

30



Page/s	Line/s	Changes
1	17	Included references.
2	1	Added emphasis that the results are just from our simulations.
2	7-10	Added values for global and European mean temperature anomalies
2	26	Altered "land use" to "land cover".
3	15-21	Included a description of natural forcings.
5	8	Added a reference to the new experimental set-up table.
9-12		Sections 3.2.1 and 3.2.3 have swapped positions.
9	31	Corrected reference
10	12-15	Included a mention of dynamics.
11	13-14	Corrected reference.
11	16	Changed "remote" to "adjacent" and rephrased.
13	18-23	Added a note on hydroclimate uncertainties
14	28-30	Moved paragraph.
15	5-21	Added more information on the temperature response of HadCM3 and on the comparison between HadCM3 and other models and palaeodata.
16	4-5	Added comparison with PMIP anomalies.
17	7-10	Stressed the advantages of regional models.
17	18-19	Added mention of climate uncertainties
17	25-31	Added comparison between HadCM3 and LUCID for albedo and heat flux responses.
17/18	33-4	Expanded comment on transient simulations.
19	17	Clarified statement on KK10 land use.
20	8	Updated value.
22-28		Updated references.
29		Included new Table 1: Experimental set-up
33		Included new Figure 4 (annual temperature anomalies)

45

Added new Figure 16 (albedo and heat fluxes)

1

2